



# *crestr* An R package to perform probabilistic climate reconstructions using fossil proxies

Manuel Chevalier<sup>1, 2</sup>

<sup>1</sup>Institute of Geosciences, Sect. Meteorology, Rheinische Friedrich-Wilhelms-Universität Bonn, Auf dem Hügel 20, 53121 Bonn, Germany

<sup>2</sup>Institute of Earth Surface Dynamics, Geopolis, University of Lausanne, Lausanne, Switzerland

**Correspondence:** Manuel Chevalier (chevalier.manuel@gmail.com)

**Abstract.** Statistical climate reconstruction techniques are practical tools to study past climate variability from fossil proxy data. In particular, the methods based on probability density functions (PDFs) are powerful at producing robust results from various environments and proxies. However, accessing and curating the necessary calibration data, as well as the complexity of interpreting probabilistic results, often limit their use in palaeoclimatological studies. To address these problems, I present a new R package (*crestr*) to apply the CREST method (Climate REconstruction SofTware) on diverse palaeoecological datasets. *crestr* includes a globally curated calibration dataset for six common climate proxies (*i.e.* plants, beetles, chironomids, rodents, foraminifera, and dinoflagellate cysts) that enables its use in most terrestrial and marine regions. The package can also be used with private data collections instead of, or in combination with, the provided dataset. It also includes a suite of graphical diagnostic tools to represent the data at each step of the reconstruction process and provide insights into the effect of the different modelling assumptions and external factors that underlie a reconstruction. With this R package, the CREST method can now be used in a scriptable environment, thus simplifying its use and integration in existing workflows. It is hoped that *crestr* will contribute to producing the much-needed quantified records from the many regions where climate reconstructions are currently lacking, despite the existence of suitable fossil records.

## 1 Introduction

Fossil-based climate reconstruction techniques are commonly used to quantify past climates and shed light on the nature of climate drivers across various spatial and/or temporal scales. Over the years, a growing number of distinct techniques of increasing complexity has been proposed, each one being based on a unique set of assumptions regarding the modelling of ecological datasets and their translation into climate parameters (*e.g.* Birks et al. (2010), Chevalier et al. (2020b)). Of this array of techniques, Weighted-Averaging (WA, ter Braak and van Dame (1989)), Weighted-Averaging Partial Least Square (WAPLS, ter Braak et al. (1993)) and the Modern Analogue Technique (MAT, Overpeck et al. (1985)) have been the most widely employed. Despite their conceptual simplicity and demonstrated capacity to reliably reconstruct climate from palaeoecological



25 datasets, the limited availability of robust calibration datasets (*i.e.* regional collections of modern proxy samples) beyond the Northern Hemisphere extratropics has, however, hindered their application in these regions, despite the existence of suitable records from all environments worldwide (Chevalier et al., 2020b).

The abundance of such un-quantified fossil pollen records from southern Africa triggered the development of the CREST (Climate REconstruction SofTware) method (Chevalier et al., 2014). Built upon from the original work of Kühl et al. (2002) — who first proposed to replace the commonly-used modern proxy samples with modern proxy geolocalised occurrence data to estimate probabilistic proxy-climate relationships — CREST estimates and combines probability density functions (PDFs) to reconstruct climate parameters. Using a private collection of modern plant occurrences held by the South African National Botanical Institute (SANBI), CREST has been successfully employed to reconstruct diverse temperature, precipitation and moisture-related variables for different time periods across the southern African tropical and subtropical regions (see for instance Chase et al. (2015b), Chase et al. (2015a), Chevalier and Chase (2015), Chevalier and Chase (2016), Lim et al. (2016), Cordova et al. (2017)). A global, multi-proxy calibration dataset containing millions of modern occurrence data was subsequently released (Chevalier, 2019) to support the use of CREST beyond southern Africa and contribute to the creation of quantified climate records worldwide (Yi et al. (2020), Hui et al. (2021)).

In addition to its broad applicability, CREST also bears some fundamental statistical properties that make it well-adapted to the analysis of palaeoecological datasets (Chevalier et al., 2020b). While techniques such as MAT or WA-PLS are primarily designed to associate modern proxy observations with their ‘most likely’ or ‘mean’ climate values only, CREST estimates, weights and propagates all the climate values that are compatible with the observed fossil data. The posterior climate reconstructions obtained from CREST can thus be understood as a weighted ensemble of all plausible climate values and not a simpler, less informative ‘most likely’ or ‘best’ climate estimate with statistical errors (see the conceptual Fig. 1). While the latter might be optimal when a sample is analysed in complete isolation, the presence of independent, local or regional information (*i.e.* other samples for the same core or independent records) usually provides additional information that may not always be consistent with such an isolated, analytical solution. In practice, joint solutions based on all the available information often differ from most likely climate estimates (Fig. 1). Using methods that can model the full range of climate uncertainties associated with a proxy sample is thus critical to bring various reconstructions and even climate simulations together in the most cohesive way.

Despite their definite advantages, uncertainty-based frameworks like CREST can be complex to employ, and their results are challenging to process and represent. To facilitate access and use of such probabilistic techniques to a broad range of non-experts, I present a new R package `crestR` that enables employing CREST and its built-in calibration dataset in a scriptable environment. In addition to its technical core, the package also contains an array of graphical diagnostic tools to represent the data at different pivotal steps of the reconstruction process and facilitate objective evaluations of the data and results. This paper is structured as follows. First, Section 2 summarises the mathematics and assumptions underpinning the approach and introduces the embedded calibration dataset. Then, Section 3 explains the philosophy and main elements of the package and describes the format of the different input files required. Finally, Section 4 documents a step-by-step guided tour of the package,

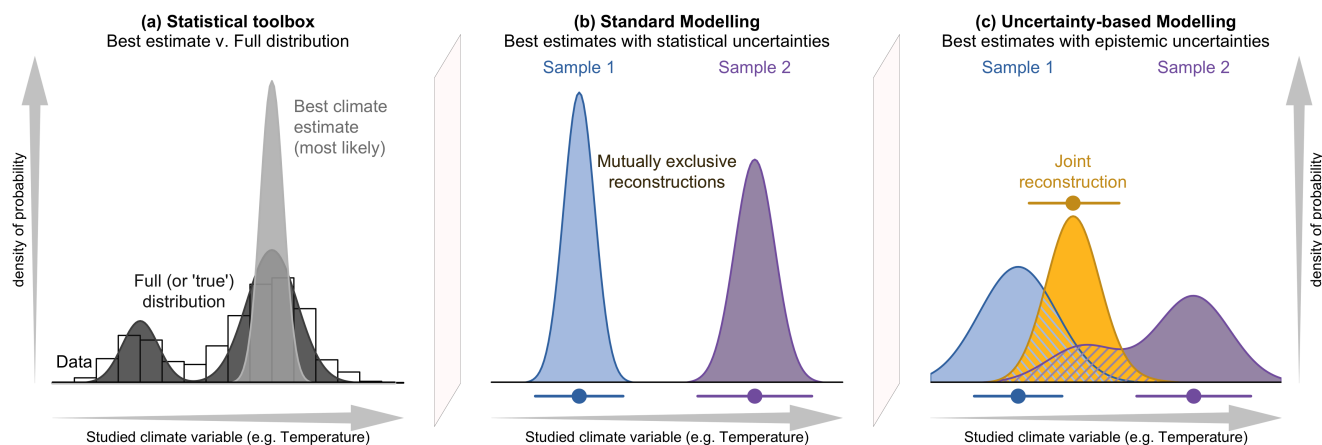


**Figure 1.** (a) Conceptual illustration of the differences between a modelling approach based on the estimation of the most likely climate where all the probabilities are concentrated around the mode (light grey), and a modelling approach focused on the full spread of the data with the probabilities more spread along the climate gradient (dark grey). In both cases, the area under the curve sums to one. The two types of approaches are illustrated in (b) and (c) with two theoretical fossil samples (in blue and purple) representing two independent reconstructions of the same climatic parameter for the same time period. (b) The two reconstructions are derived from a method focused on only estimating the most likely climate value, resulting in 'apparently' incompatible reconstructions. (c) The same samples are reconstructed using an approach that estimates their complete uncertainty distributions. In this case, the response of the blue sample is broader, and the response of the purple sample becomes bimodal. When the full spread of these uncertainties is considered, the two reconstructions are not incompatible anymore, and a joint climate estimate (gold) can be derived from their overlapping sections (hashed polygons).

illustrating the successive stages of a CREST analysis and how to use the diagnostic tools to reproduce a recently published pollen-based temperature reconstruction (Chevalier et al., 2021).

## 2 CREST method & Calibration data

### 60 2.1 The probability density function (PDF) approach

As is standard with statistical climate reconstruction techniques, the core process of CREST can be decomposed into two major stages: 1) estimating the modern climatic responses of the proxies observed in the fossil sequence (Fig. 2a-c) and 2) combining these responses to reconstruct past climates (Fig. 2d). In the following sections, the main elements of these two stages are presented along with all the parameters and/or modelling assumptions that can be modified in `crestr`. For an  
65 in-depth description of the method and its assumptions, the reader is, however, referred to .

As is standard with statistical climate reconstruction techniques, the core process of a CREST reconstruction can be decomposed into two major stages: 1) estimating the modern climatic responses of the proxies observed in the fossil sequence (Fig. 2a-c) and 2) combining these responses to reconstruct past climates (see Fig. 2d). The main elements of these two stages are

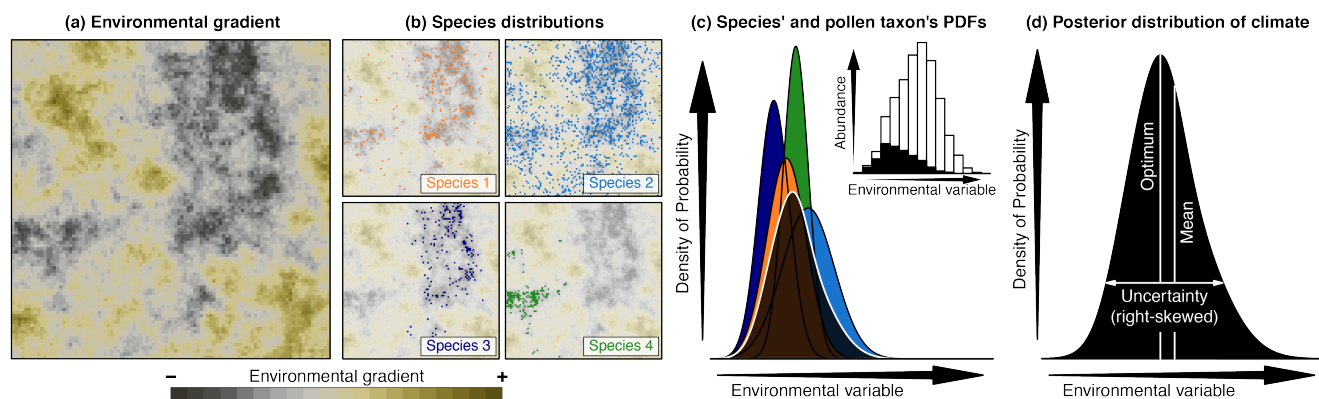


**Figure 2.** Conceptual representation of CREST using artificial pollen data. (a) Spatial distribution of a climate variable to reconstruct (e.g. temperature). (b) Occurrences of four species part of the same pollen group exhibiting marked preferences for the lowest values of that climate (e.g. dark/cold values) cross the study area. (c) Combination of the four species PDFs (colours) into the pollen PDF (black). The histogram represents the proportion of the modern climate space (white) occupied by at least one of the four species (black), highlighting the higher chances of observing the taxon at the lower end of the climate gradient. (d) Example of a posterior climate distribution resulting from the multiplication of PDFs and the type of synthetic statistics (e.g. optimum, mean, uncertainty range) one can derive from it.

presented in the following sections, along with all the parameters and/or modelling assumptions that can be modified in ‘crestr.,

70 For an in-depth description of the method and its assumptions, the reader is, however, referred to Chevalier et al. (2014).

### 2.1.1 Stage 1: Modelling the proxy-climate relationships

In CREST, PDFs are used to transform the information contained in the modern observations of biological climate proxies into probabilistic climate responses. A PDF thus represents a weighted ensemble of all the conditions where the proxy is observed today. PDFs can be fitted in one or two steps depending on the nature and taxonomic resolution of the studied proxy. Climate responses are first fitted at the species level (hereafter  $\text{PDF}_{\text{sp}}(c, s)$  with  $c$  representing the studied climate variable and  $s$  a species), and when necessary, these  $\text{PDF}_{\text{sp}}(c, s)$  are then combined together to meet the taxonomic resolution of the fossil taxon (hereafter  $\text{PDF}_{\text{tx}}(t, c)$  with  $t$  representing the observed taxon).

For all the species, their empirical mean climate and associated variance are calculated from their modern distributions following Eq. 1 and 2. These two parameters can be intuitively interpreted as the climate preference and tolerance of the species. For a robust estimation, it is recommended to exclude species with too few observations. Different studies have shown that a threshold of a minimum of  $N_s \geq 20$ -25 distinct occurrences usually leads to robust estimates (e.g. Chevalier et al. (2014), Chevalier et al. (2021)). However, this number can vary between regions and climates. Each observation can also be weighted to account for the uneven distribution of modern climate (Kühl et al. (2002), Bray et al. (2006)). Extreme values are usually under-represented (see, for instance, the inset histogram on Fig. 2c), and this bias can push the estimation of the  $\text{PDF}_{\text{sp}}(c, s)$  towards the mean climate observed across the study area (i.e. towards the centre of the “climate space”). It can also artificially

85



shrink the posterior range of the reconstructions. In CREST, this weighting can be accounted for by first sorting the  $N$  climate values that compose the climate space into bins of equal sizes (*e.g.*  $2^\circ\text{C}$  or  $50\text{ mm}$ ). Then, each climate value is given a weight defined as the inverse of the abundance of the bin it belongs to (Eq. 3). With this correction, abundant climate values are down-weighted, while the rarer ones are up-weighted, and the distribution of modern climate is more ‘balanced’.

$$90 \quad \bar{m}_{s,c} = \frac{1}{\sum_i k(c_i)} \sum_{i=1}^{N_s} k(c_i) c_i \quad (1)$$

$$s_{s,c}^2 = \frac{1}{\sum_i k(c_i)} \sum_{i=1}^{N_s} k(c_i) (c_i - \bar{m}_{s,c})^2 \quad (2)$$

$$k(c_j) = \left( \frac{1}{N} \sum_{i=1}^N \mathbf{1}_{c_i \in \text{bin}_{c_j}} \right)^{-1} \quad (3)$$

These two parameters,  $\bar{m}_{s,c}$  and  $s_{s,c}$ , are used to define a regular, unimodal distribution for the  $\text{PDF}_{\text{sp}}(s, c)$ . In CREST, the shape of these distributions is pre-defined to be either normal (Eq. 4) or log-normal (Eq. 5). The decision should be made based on the climate variable to reconstruct. In general, log-normal distributions are recommended for variables that are undefined for negative values, such as precipitation variables.

$$\text{PDF}_{\text{sp}}(s, c) = \frac{1}{\sqrt{2\pi s_{s,c}^2}} \exp\left(-\frac{(c - \bar{m}_{s,c})^2}{2s_{s,c}^2}\right) \quad (4)$$

$$\text{PDF}_{\text{sp}}(s, c) = \frac{1}{\sqrt{2\pi\sigma^2 c^2}} \exp\left(-\frac{(\ln(c) - \mu)^2}{2\sigma^2}\right) \quad (5)$$

$$\text{with} \begin{cases} \mu = \ln(\bar{m}_{s,c}) - \frac{1}{2} \ln\left(1 + \frac{s_{s,c}^2}{\bar{m}_{s,c}^2}\right) \\ \sigma^2 = \ln\left(1 + \frac{s_{s,c}^2}{\bar{m}_{s,c}^2}\right) \end{cases}$$

100 Finally, the  $\text{PDF}_{\text{sp}}(s, c)$  of the  $S(t)$  species composing taxon  $t$  are linearly combined to create the climate response of taxon  $t$  to climate variable  $c$  (Eq. 6). This linear combination ensures that all the climate values that support the presence of at least one species have a non-null probability in the  $\text{PDF}_{\text{tx}}(t, c)$ . Contrary to the previous step, no additional constraints are added here. The distribution of the  $\text{PDF}_{\text{tx}}(t, c)$  can thus be asymmetrical and even multimodal if different (groups of) composing species exhibit distinct climate requirements. An additional option is to weigh the different  $\text{PDF}_{\text{sp}}(s, c)$  by the square root of  
 105 the number of individual grid cells composing their distribution ( $N_s$ ). Considering that it is harder to estimate robust parameters with few points, this weighting gives more importance to the species with more extensive geographical distributions today, or, to say it differently, it gives more weight to the species whose climate responses can be the most robustly defined.



$$\text{PDF}_{\text{tx}}(t, c) = \frac{1}{\sum_s \sqrt{N_s}} \left( \sum_{s=1}^{S(t)} \sqrt{N_s} \text{PDF}_{\text{sp}}(s, c) \right) \quad (6)$$

### 2.1.2 Stage 2: Reconstructing climate

110 With the  $\text{PDF}_{\text{tx}}(t, c)$  calibrated, posterior climate reconstructions can be estimated from their multiplication (Eq. 7, where  $z$   
 represents the age or depth of the sample to reconstruct, and Fig. 2d). Due to their exponential nature, the  $\text{PDF}_{\text{tx}}(t, c)$  rapidly  
 converge to zero beyond the range of the modern observations of its composing species. As such, the multiplication of these  
 $\text{PDF}_{\text{tx}}(t, c)$  ensures that only the climate values where all the taxa can coexist have a non-null (or, more precisely, a non-  
 infinitesimal) probability. In addition, the presence or absence of each taxon is considered independent from the others. As  
 115 such, it is possible to select a subset of climatically sensitive taxa to reconstruct each climate variable and maximise the  
 reconstruction signal (Chevalier and Chase, 2015), even if it is not always mandatory (Chevalier et al., 2021). These definitions  
 of sensitive taxa are always specific to a specific region and variable and should not be generalised (Chevalier et al., in press).

$$\text{PDF}_{\text{restructn}}(c, z) = \left( \prod_{t=1}^{T(z)} \text{PDF}_{\text{tx}}(t, c)^{\omega(t, z)} \right) (\sum_t \omega(t, z))^{-1} \quad (7)$$

Finally, the selected  $\text{PDF}_{\text{tx}}(t, c)$  can be weighted with the parameter  $\omega(t, z)$ , which can take any positive values. For pres-  
 120 ence/absence observations, the weights of taxon  $t$  will be either one (the taxon is observed) or zero (the taxon is not observed).  
 For compositional data, the weights can be the observed percentages (*i.e.* values between 0 and 100) or rescaled percentages  
 when the observed percentages are not directly proportional to the taxa composition across the catchment. In most cases, us-  
 ing raw percentages to weight taxa can give considerable weight to abundant, ubiquitous taxa that do not have a well-defined  
 climate response and strongly limit the influence of rarer taxa with more explicit climate preferences.

125 An empirical normalisation is proposed in CREST to account for the varying production rates, distribution and preservation  
 processes impacting the relative proportions of fossil taxa observed in the sediments (Chevalier et al., 2014). This scaling entails  
 calculating the average percentage of each taxon when it is present and dividing all its percentages by this taxon-specific scaling  
 factor (Eq. 8, where  $O(t, z)$  represents the observed percentage of taxon  $t$  at age or depth  $z$ ). With this normalisation, all the  
 taxa vary on a standardised scale. The average presence is given a weight of 1, and values below and above this average  
 130 presence threshold are assumed to represent lower and higher abundance in the environment. While the empirical nature of  
 this solution makes it imperfect and sensitive to the quality of the data, it nevertheless enables using percentages to inform  
 the reconstructions. One alternative solution is to convert the percentages to presence and absence, but this approach can be  
 limiting when most of the observed variability concerns changes in the relative proportions of different taxa, rather than a clear  
 succession of taxa with different climate requirements (see for instance the pollen diagram in Chase et al. (2015b)). These  
 135 different weighting options are available in crestr, but users can also provide a weighting strategy of their design to better  
 account for the specificity of their data.



$$\omega(t, z) = \frac{O(t, z)}{(\sum_z O(t, z)) / (\sum_z \mathbf{1}_{O(t, z) > 0})} \quad (8)$$

## 2.2 CREST calibration dataset

A multiproxy calibration dataset to estimate PDFs from a global collection of geolocalised presence-only data (hereafter proxy  
140 distributions) was first presented in Chevalier (2019). These data were obtained from the Global Biodiversity Information  
Facility (GBIF) database, an online collection of geolocalised observations of biological entities (GBIF, 2018). The calibration  
dataset (hereafter *gbif4crest*, Chevalier, 2020) contains the species distributions of six common palaeoecological fossils: the  
five taxa presented in the original version of the dataset — plants (GBIF (2020l), GBIF (2020h), GBIF (2020k), GBIF (2020f),  
GBIF (2020g), GBIF (2020m), GBIF (2020i), GBIF (2020n), GBIF (2020j), GBIF (2021a), GBIF (2021b)) for fossil pollen  
145 and macrofossils, chironomids (GBIF, 2020b), beetles (GBIF, 2020a), diatoms (GBIF, 2020c) and foraminifera (GBIF, 2020d)  
– to which rodents (GBIF, 2020e) were recently added (Fig. 3). These data were curated and stored in a relational database to  
ensure the consistency of the data.

The coordinates of all the presence records of these six common palaeoecological fossil proxies were upscaled at a spatial  
150 resolution of  $0.25 \times 0.25^\circ$  (hereafter QDGC for Quarter-Degree Grid Cell). They were subsequently associated with  
terrestrial and oceanic environmental variables at the same resolution ((Fick and Hijmans (2017), Zomer et al. (2008), Locarnini  
et al. (2019), Zweng et al. (2018), Garcia et al. (2019a), Garcia et al. (2019b), Reynolds et al. (2007), see details in Tables 1 and  
2). The QDGC spatial resolution is an empirical trade-off between numerous factors, including the resolution of the presence  
data, the quality of the data or the spatial representativity of the studied proxy (see discussions in Chevalier et al. (2014) and  
Chevalier (2019)). However, this trade-off may be suboptimal in some situations, and for that reason, *crest* can also be  
155 used with the raw GBIF data and even alternative calibration datasets.

In its current version (V2), the *gbif4crest* calibration dataset contains about 25.3 million unique presence data for the six  
proxies. Unfortunately, the density of data available varies between proxies and regions (Fig. 3). Plant data dominate the  
calibration dataset (>22 million unique occurrences) and allow for the use of *crest* across all landmasses where vegetation  
currently grows. For the five other proxies, the calibration data are not as extensive. However, these datasets are regularly  
160 updated by GBIF. For example, the first version of the *gbif4crest* dataset released in 2018 contained about 17.5 million QDGC  
entries, while the new version contains approximately 25.3 million entries (~44% increase). The range of ‘reconstructible’  
areas is thus rapidly broadening (see, for instance, the coverage of Russia by plant data compared to the first version of the  
*gbif4crest* dataset presented in Chevalier (2019)).

The *gbif4crest* database is composed of three main types of data: taxonomic data (TAXA table on Fig. 4), distribution  
165 data (DISTRIB and DISTRIB\_QDGC tables) and diverse geopolitical, climatological, and environmental data (DATA\_QDGC  
table). Its structure is slightly different from the first version presented in Chevalier (2019), with a grouping of all the sep-  
arate QDGC tables in a unique DATA\_QDGC table to enable faster data extraction. In addition, various environmental and  
geographical descriptors were also introduced to characterise each grid cell and allow a more refined data selection. These in-  
clude elevation and elevation variability (Amante and Eakins, 2009), the country (<https://www.natureearthdata.com>) or ocean



Number of occurrence data per grid cell for six common biological climate proxies

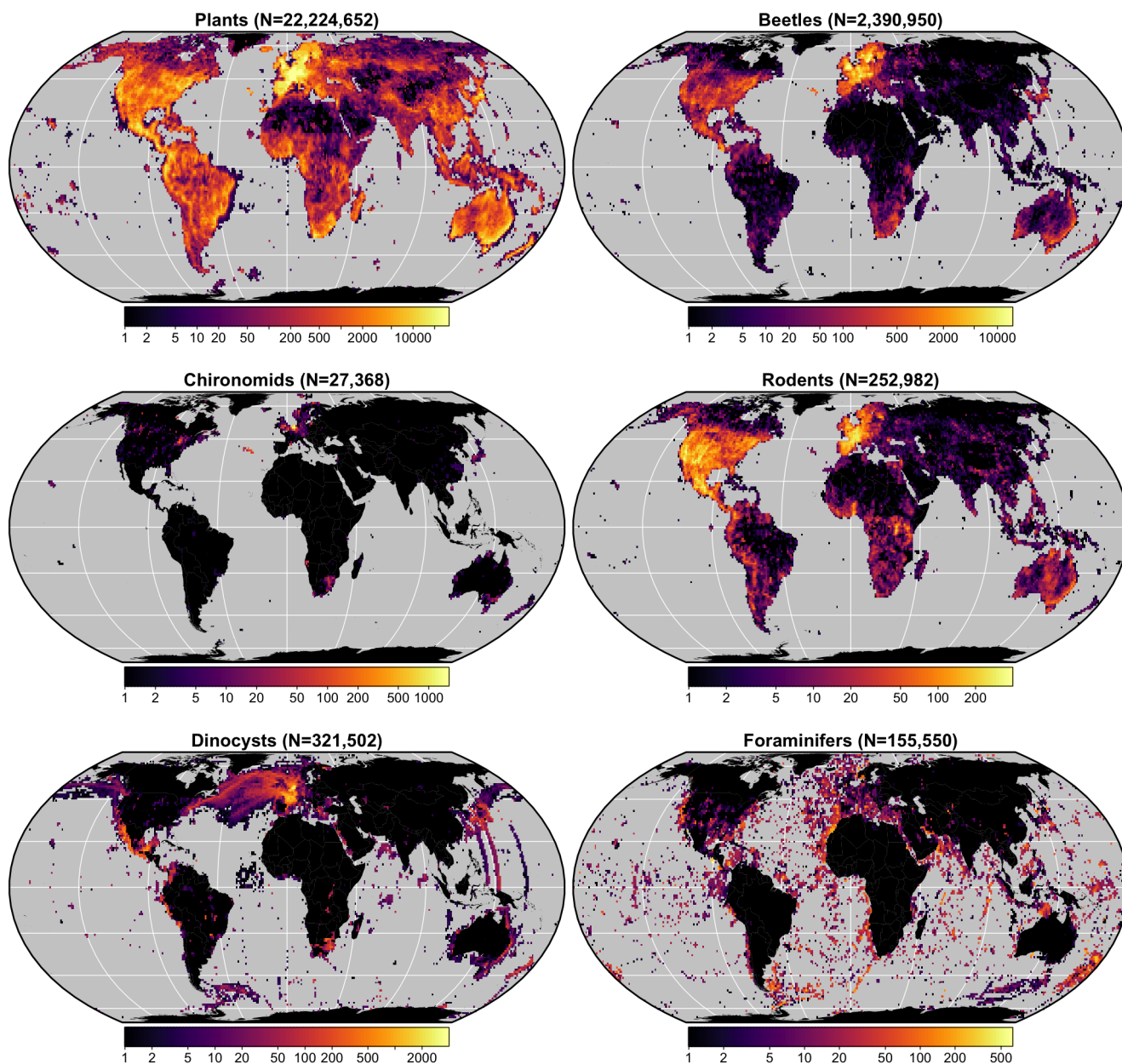


**Figure 3.** Data density of the six climate proxies available in the gbif4crest calibration database. The total number of unique species occurrences (N) is indicated for each proxy. The maps are based on the ‘Equal Earth’ map projection to better account for the relative sizes of the different continents.





**Table 1.** List of terrestrial variables available in the gbif4crest database. Each one can be selected in crestr using its associated code. List of abbreviations: (Temp.) Temperature, (Precip.) Precipitation.

Terrestrial variables		
Code	Full name	Source
bio1	Mean Annual Temp. (°C)	Fick and Hijmans (2017)
bio2	Mean Diurnal Range (°C)	Fick and Hijmans (2017)
bio3	Isothermality (x100)	Fick and Hijmans (2017)
bio4	Temp. Seasonality (standard deviation x100) (°C)	Fick and Hijmans (2017)
bio5	Max Temp. of the Warmest Month (°C)	Fick and Hijmans (2017)
bio6	Min Temp. of the Coldest Month (°C)	Fick and Hijmans (2017)
bio7	Temp. Annual Range (°C)	Fick and Hijmans (2017)
bio8	Mean Temp. of the Wettest Quarter (°C)	Fick and Hijmans (2017)
bio9	Mean Temp. of the Driest Quarter (°C)	Fick and Hijmans (2017)
bio10	Mean Temp. of the Warmest Quarter (°C)	Fick and Hijmans (2017)
bio11	Mean Temp. of the Coldest Quarter (°C)	Fick and Hijmans (2017)
bio12	Annual precip. (mm)	Fick and Hijmans (2017)
bio13	Precip. of the Wettest Month (mm)	Fick and Hijmans (2017)
bio14	Precip. of the Driest Month (mm)	Fick and Hijmans (2017)
bio15	Precip. Seasonality (Coefficient of Variation) (mm)	Fick and Hijmans (2017)
bio16	Precip. of the Wettest Quarter (mm)	Fick and Hijmans (2017)
bio17	Precip. of the Driest Quarter (mm)	Fick and Hijmans (2017)
bio18	Precip. of the Warmest Quarter (mm)	Fick and Hijmans (2017)
bio19	Precip. of the Coldest Quarter (mm)	Fick and Hijmans (2017)
ai	Aridity Index (unitless)	Zomer et al. (2008)

170 (https://www.marinerregions.org) names, as well as different levels of ecological classification for the terrestrial (Olson et al., 2001) and marine (Costello et al., 2017) realms. The first and last observation dates are also now included, along with the type of observation, as reported by GBIF (see `DISTRIB_QDGC` table on Fig. 4). Finally, the `DATA_QDGC` table was entirely recalculated using a new protocol that better accounts for coastal margins, implying that some coastal climate values will differ, however marginally, between the different versions of the gbif4crest dataset.

175 Due to its large size (about 15 Gb), this database is not downloaded when installing the package, but it can be accessed in different ways. First, the data are stored in an open-access, cloud-based PostgreSQL database that can be accessed via `crestr`. This solution is the recommended option, as users without any SQL knowledge can benefit from the package's interface to automatically query the database by providing study-specific parameters (*e.g.* the name of the taxa or geographical boundaries for the study area) to import all the necessary data in the correct format to the R environment (see Section 4.2). Second,  
 180 advanced users can also directly query the database to extract and curate data from the `DISTRIB` or `DISTRIB_QDGC` tables



**Table 2.** List of marine variables available in the *gbif4crest* database. Each one can be selected in *crestr* using its associated code. List of abbreviations: (SST) Sea Surface Temperature, (SSS) Sea Surface Salinity.

Oceanic variables		
Code	Full name	Source
sst_ann	Mean Annual SST (°C)	Locarnini et al. (2018)
sst_jfm	Mean Winter SST (°C)	Locarnini et al. (2018)
sst_amj	Mean Spring SST (°C)	Locarnini et al. (2018)
sst_jas	Mean Summer SST (°C)	Locarnini et al. (2018)
sst_ond	Mean Fall SST (°C)	Locarnini et al. (2018)
sss_ann	Mean Annual SSS (PSU)	Zweng et al. (2018)
sss_jfm	Mean Winter SSS (PSU)	Zweng et al. (2018)
sss_amj	Mean Spring SSS (PSU)	Zweng et al. (2018)
sss_jas	Mean Summer SSS (PSU)	Zweng et al. (2018)
sss_ond	Mean Fall SSS (PSU)	Zweng et al. (2018)
icec_ann	Mean Annual Sea Ice Concentration (%)	Reynolds et al. (2007)
icec_jfm	Mean Winter Sea Ice Concentration (%)	Reynolds et al. (2007)
icec_amj	Mean Spring Sea Ice Concentration (%)	Reynolds et al. (2007)
icec_jas	Mean Summer Ice Concentration (%)	Reynolds et al. (2007)
icec_ond	Mean Fall Sea Ice Concentration (%)	Reynolds et al. (2007)
diss_oxy	Dissolved Oxygen Concentration (µmol/L)	Garcia et al. (2018a)
nitrate	Nitrate Concentration (µmol/L)	Garcia et al. (2018b)
phosphate	Phosphate Concentration (µmol/L)	Garcia et al. (2018b)
silicate	Silicate Concentration (µmol/L)	Garcia et al. (2018b)

using the `dbRequest()` function and subsequently associate these data with climate variables. Finally, the full *gbif4crest* calibration dataset can be downloaded as an SQLite3 portable database file from Chevalier (2020).

### 3 The *crestr* R package

#### 3.1 Philosophy of the package

185 The *crestr* package has been designed for two independent but complementary modelling purposes. The probabilistic proxy-climate responses can be used to quantitatively reconstruct climate from their statistical combination, such as in Chevalier et al. (2021) or Chevalier and Chase (2015), or, alternatively, they can be used in a more qualitative way to determine the (relative) climate sensitivities of different taxa in a given area to characterise past ecological changes, such as in Chevalier et al. (in press) or Quick et al. (2021). For a simpler access to the different functionalities, default values are provided for all parameters  
 190 to enable a rapid generation of preliminary results that users can then use as a starting point to fine-tune the model to their

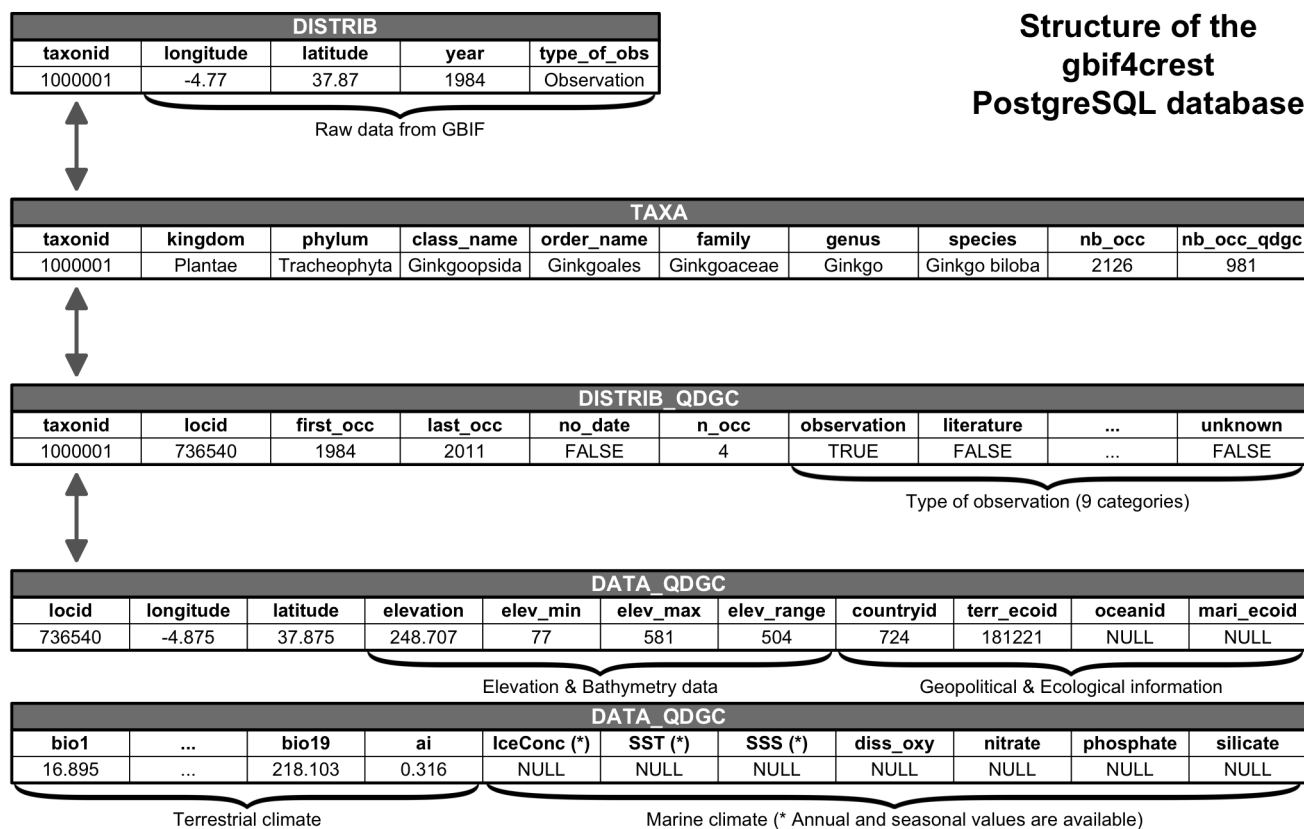


**Figure 4.** Structure of the gbif4crest PostgreSQL database. By default, the package extracts data from the TAXA, DISTRIB-QDGC and DATA-QDGC tables. The DISTRIB table contains the raw occurrence data obtained from GBIF and can be used to process the data at a different spatial resolution.

data. To guide users in this task and avoid the common ‘black box’ criticism faced by many complex statistical tools, a large array of publication-ready, graphical diagnostic tools was designed to automatically represent CREST data in a standardised way. These tools include plots of the calibration data, the estimated climate responses, the reconstructions and more. They can be used to look at the data from different perspectives to help interpret the results, and possibly to help identify potential issues or biases in the selected data and/or parameters. Such diagnostic tools are available for every stage of the process and, as exemplified in section 4, they can be generated with a single line of R code.

### 3.2 The central element: the `crestObj` object

In `crestr`, all the CREST-related data are stored within a single S3 object of the class `crestObj`. Most functions of the package will take a `crestObj` as their main input and will return an updated version of that object. In practice, a `crestObj` is a nested list that contains five sub-lists, each one grouping a specific type of information, such as the calibration data, the

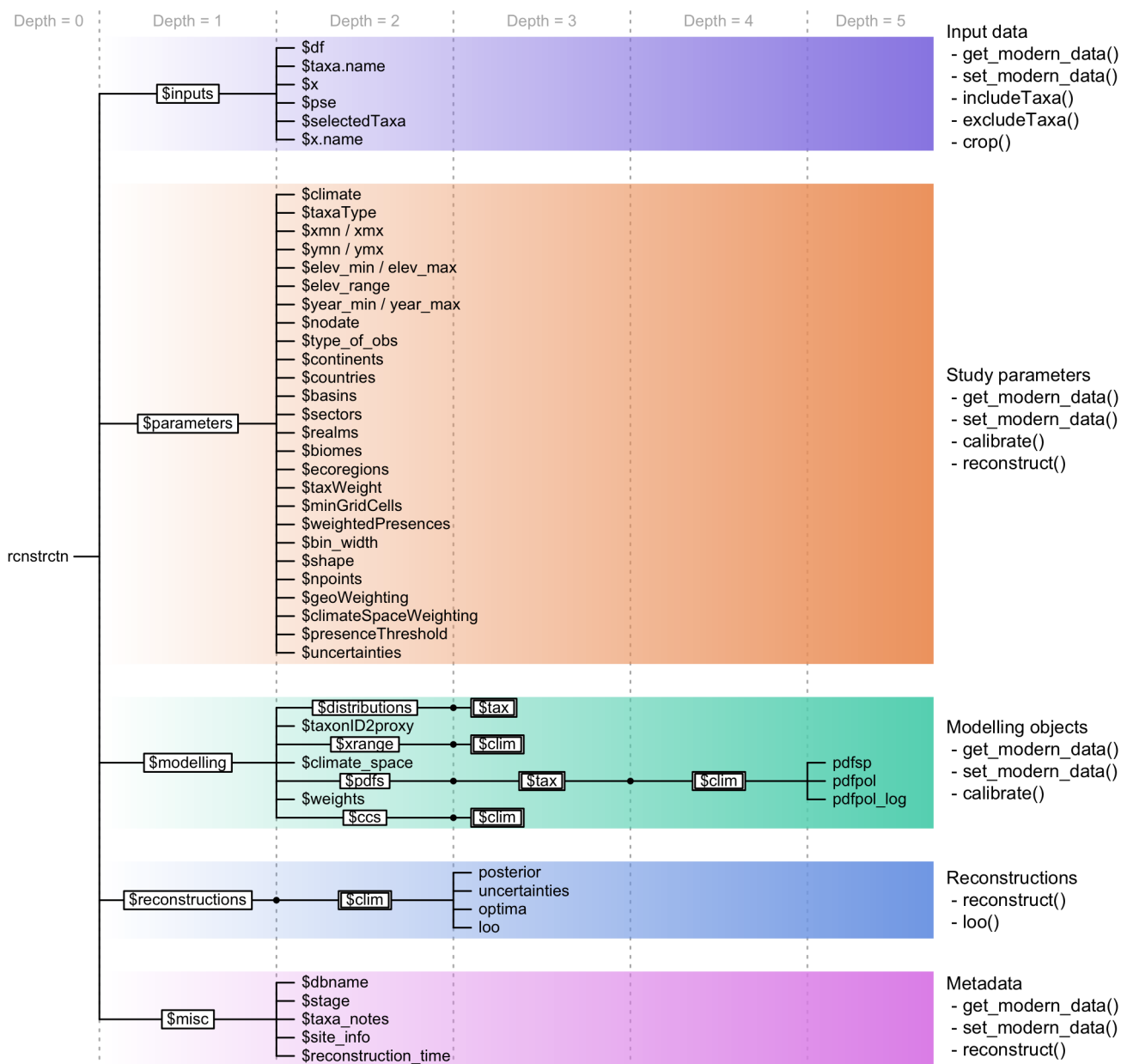


**Figure 5.** Structure of a crestObj, here called 'rcnstrctn', with the five main sub-lists in colour. For simplicity, lists with many elements ('tax' or 'clim') are represented with double framed boxes. The unframed terminal nodes on the right-hand side of each branch are simple R objects, such as numbers, characters, vectors or data frames. The names of the functions that modify the objects in the sub-lists are indicated on the right.



fitted climate responses, and the reconstructions (Fig. 5). Wrapper functions have been implemented to manipulate and/or modify the information contained in a `crestObj` so that, users are never expected to manually modify their `crestObj` — even if it is possible. The five sub-lists contain the following information:

- `inputs`: contains the raw data (*e.g.* the counts/percentages, the ages of the samples or the names of the fossil taxa).
- 205 – `parameters`: contains the parameters provided at the different stages of the analysis (*e.g.* the data extraction or the fitting and combination of the PDFs)
- `modelling`: contains all the data related to the estimation of the PDFs (*e.g.* the distribution data for calibration, the climate space or the PDFs themselves).
- `reconstructions`: contains all the results (*e.g.* best estimates, synthetic error measurements as well as the full  
210 posterior distribution of the uncertainties).
- `misc`: contains some additional metadata relative to the reconstruction (*e.g.* the site location or, most importantly, information relative to the proxy-species equivalency described in section 3.3.2).

### 3.3 Input data for `crestr`

Five different input data files are compatible with `crestr`. However, most applications will only require two file (the `df` and `PSE`  
215 files, see below) to be created. More specific applications may require up to four of these files. All the files can be prepared outside the R environment and imported using standard R functions.

#### 3.3.1 The fossil data (`df`)

The `df` data frame is only required if `crestr` is used for reconstructing climate and can be omitted if the objective is limited to modelling the climate response(s) of different taxa. `df` should be a data frame with the different samples entered as rows,  
220 with either the age, depth, or sample ID as the first column and the fossil data in the subsequent columns. `df` can contain raw counts, percentages, presence/absence (1s and 0s) or even relative weights to be used in the reconstruction (see examples in Section 4.5).

#### 3.3.2 The proxy-species equivalency (`PSE`) table

The `PSE` data frame is required to use the `gbif4crest` calibration dataset. It is used to associate fossil taxon names to the species  
225 distributions of various species stored in the `TAXA` and `DISTRIB_QDGC` tables (Fig. 4). When all the fossil taxa are identified at the species level, the `PSE` table should be a simple data frame with one row per taxon. In most cases, however, fossil taxa are identified at a higher taxonomic level (sub-genus, genus, sub-family, family). These varying levels of identification should be encoded in the `PSE` file to link one or more (groups of) species to their common fossil taxon name.

In practice, a `PSE` file is composed of five columns (Table 3). The first one (*Level*) contains an integer that indicates the level  
230 of taxonomic resolution of the row (1 for Family, 2 for Genus, 3 for Species and 4 for taxa that should be excluded from the



**Table 3.** Example classification of four pollen taxa from the example case study, each one with a different level of taxonomic resolution. The last column ‘Taxonomic resolution’ is added here for explanatory purposes only and is not required in a real ‘PSE’ table.

Level	Family	Genus	Species	ProxyName	Taxonomic resolution
1	Asteraceae			Asteraceae undiff.	Family
2	Asteraceae	<i>Stoebe</i>		<i>Stoebe</i> -type	Subfamily
2	Asteraceae	<i>Elytropappus</i>		<i>Stoebe</i> -type	Subfamily
2	Asteraceae	<i>Artemisia</i>		<i>Artemisia</i>	Genus level
3	Areaceae	<i>Elaeis</i>	<i>Elaeis guineensis</i>	<i>Elaeis guineensis</i>	Species
4				Triletes spores	To be excluded

reconstruction, e.g. ‘Triletes spores’ in the example case study below). The fifth column *ProxyName* contains the name of the taxon and columns two to four contain the taxonomic classification of that taxon as *Family*, *Genus* and *Species*, respectively. For simplicity, a pre-formatted version of the PSE table with the names of all the taxa to study can be generated by `crestr` using the `createPSE(list_of_taxa)` function that generates a spreadsheet with the correct structure and with the Level and ProxyName columns automatically filled in.

When performing the species to proxy classification with the `crest.get_modern_data()` function (see Section 4.2), `crestr` first classifies the taxa with the lowest taxonomical resolution (i.e. when *Level* is equal to one), and then increases the resolution *Level* by *Level*. In the example in Table 3, different taxonomic resolution levels are provided for different plant species belonging to the highly diverse Asteraceae family (the daisy family). To distribute all the Asteraceae species observed across the study area to their appropriate category, all the species are first classified as ‘Asteraceae undiff.’. In a second time, the classification of some of these Asteraceae species is refined when reaching the better resolved sub-groups (*Stoebe*-type and *Artemisia* at *Level* 2). At the end of the process, the ‘Asteraceae undiff.’ group only contains Asteraceae species that grow in the study area but are not part of the genera *Stoebe*, *Elytropappus* or *Artemisia*. The latter are categorised separately as *Stoebe*-type or *Artemisia*. Additional taxa can also be included to the PSE file to exclude species that are known to not be part of a group. For instance, this could have been used to simplify the climate response of the ‘Asteraceae undiff.’ group by excluding more species from it, even if the pollen grains corresponding to these species have not been observed. This categorisation process can be time-consuming, as all the taxa must be classified in a unique PSE table, and will often require many iterations to be optimised. The results of the different assignments are stored in the `crestObj` returned by the `crest.get_modern_data()` function and can be evaluated by checking `rcnstrctn$misc$taxa_notes`.

### 3.3.3 The alternative modern calibration dataset (distributions)

Users that prefer fitting proxy-climate relationships from their personal calibration data instead of the proposed *gbif4crest* dataset should prepare a `distributions` dataset following the specific structure presented in Table 4. The first two columns



255 should contain the species names (or unique identifiers) and the corresponding proxy name, respectively. If more than one species correspond to one taxon, the PDFs will be fitted in two steps, as explained in section 2.1. The following two columns contain the coordinates of the species occurrence data. Finally, the last columns contain the climate values to be reconstructed. An optional column called `weight` can be added to `distributions` in fifth position (*i.e.* between the coordinates and the climate variables) if one wants to weight the different observations. For example, the (relative) abundance of taxa observed from modern proxy samples can be used when fitting the PDFs to give more importance to the observations where that abundance is highest.

**Table 4.** Template for the `distributions` data frame. The weights column, here indicated with a '\*', is optional and can be omitted or its values all set to 1 to assign the same weight to each observation. The number of rows of the table should correspond to the number of unique occurrences available.

Species name	Taxon Name	Longitude	Latitude	Weight*	clim_1	...	clim_n
<i>Stoebe plumosa</i>	<i>Stoebe</i> -type	18.875	-34.375	20	15.8	...	711
<i>Elytropappus rhinocerotis</i>	<i>Stoebe</i> -type	18.375	-33.625	32	16.9	...	477
...	...	...	...	...	...	...	...
<i>Elaeis guineensis</i>	<i>Elaeis guineensis</i>	-4.375	10.875	4	27.4	...	1020

### 260 3.3.4 The `climate_space` data frame

This data frame is only necessary if the users use a personal calibration dataset instead of the `gbif4crest` dataset. It will enable the use of the climate space weighting (Section 2.1.1). Its structure is straightforward, with the first two columns containing longitudes and latitudes and the subsequent columns the climate variables to reconstruct. The spatial resolution and the ordering of the climate variables should be identical to the `distributions` table (Table 4).

### 265 3.3.5 The `selectedTaxa` data frame

The last data frame that may be used to inform the reconstruction is a data frame of ones and zeros called `selectedTaxa`. This data frame has as many rows and columns as there are taxa and climate variables, respectively. Each entry should be either 1 or 0 and is used to indicate if the taxon should be used to reconstruct the climate variable (value = 1) or not (value = 0). If it is not provided, a default `selectedTaxa` data frame with all entries set to 1 is added to the `crestObj`.  
 270 Users can modify this information at any point using the `includeTaxa()` and `excludeTaxa()` built-in functions. The `crest.get_modern_data()` function also modifies this data frame by setting the value to -1 when the PSE classification failed for a taxon or when the amount of data in the study area is insufficient to fit a reliable PDF (see the parameters description in section 4.2).



### 3.4 Package dependencies

275 The `crestr` package is built in R (R Core Team, 2020) using the `devtools` package (Wickham et al., 2020). `crestr`  
depends on numerous packages, including: `clipr` (Lincoln, 2020), `DBI` (R Special Interest Group on Databases (R-SIG-DB)  
et al., 2021), `openxlsx` (Schauberger and Walker, 2020), `pals` (Wright, 2021), `plot3D` (Soetaert, 2021), `plyr` (Wickham,  
2011), `raster` (Hijmans, 2021), `rgdal` (Bivand et al., 2021), `rgeos` (Bivand and Rundel, 2020), `RPostgres` (Wickham  
et al., 2021), `scales` (Wickham and Seidel, 2020), `sp` (Pebesma and Bivand, 2005, Bivand et al. (2013)), `stringr` (Wick-  
280 ham, 2019) and `viridis` (Garnier et al., 2021). The dedicated documentation, tutorials and application examples found at  
<https://mchevalier2.github.io/crestr> were generated and formatted by the package `pkgdown` (Wickham and Hesselberth, 2020).

## 4 Step-by-step user guide for `crestr`

### 4.1 Example application: Pollen-based Mean Annual Temperature reconstructions from marine core MD96-2048

To illustrate the different ways of using `crestr` and its graphical diagnostic tools, I use pollen data that were recently analysed  
285 with the original CREST software to reconstruct mean annual temperature (MAT) from marine core MD96-2048. The core  
was retrieved off the coast of South Africa and Mozambique near the mouth of the Limpopo River, and the terrestrial sediments  
are expected to come from the entire catchment of the Limpopo River, as well as the smaller local river catchments (Dupont  
et al. (2019), Dupont et al. (2011), Castañeda et al. (2016)). The MAT reconstruction is based on 181 fossil pollen samples and  
more than 150 terrestrial pollen taxa and covers the last 790,000 years. As the catchment of these marine sediments is large,  
290 an extensive calibration dataset covering all vegetation zones from tropical Africa to the temperate southwestern tip of South  
Africa was designed to prevent any artificial reduction in the possible range of variability of the reconstruction. The glacial-  
interglacial trends and amplitude of the MAT reconstructions were validated by comparing them with regional temperature  
records and other global indicators of glacial-interglacial temperature variability (*e.g.* Antarctic temperature or global sea-level  
curves, see Chevalier et al. (2021) for more details). Here, I reproduce this reconstruction using the original parameterisation  
295 of the CREST algorithm to showcase how it can easily be replicated in a few lines of code with the `crestr` package. Due to  
the update of the climate data of the calibration dataset described in section 2.2, marginal differences in the order of tenths of  
Celsius degrees can, however, be observed between the original publication and this reproduction. All the necessary datasets  
and R code are available as supplementary material.

### 4.2 Formatting the calibration data in a `crestObj`

300 As the `gbif4crest` dataset was used to fit the PDFs, using the function called `crest.get_modern_data()` is required to  
extract the calibration data from the new cloud-based `gbif4crest` calibration database. All the parameters of the function were  
defined by the characteristics of the proxy (pollen), the climate to reconstruct (MAT / bio1) and the definition of the study  
area (East and southern Africa) and are reproduced here. In addition, the three input files (*i.e.* `df`, `PSE` and `selectedTaxa`)  
required to realise this reconstruction (see section 3.3) are reproduced from the published dataset (Chevalier et al., 2020a). The





305 following points describe the different parameters of the `crest.get_modern_data()` and how they relate to the data extraction and modelling.

– The parameter `taxaType` is used to choose the type of proxy used and takes a value between 1 to 6 for plants (*i.e.* pollen and plant macroremains), beetles, chironomids, foraminifers, diatoms and rodents, respectively.

310 – The name(s) or code(s) of the `climate` variables to study should be provided here (see Tables 1 and 2 or use the function `accClimateVariables()` for a list of accepted values). Here, ‘`bio1`’ means mean annual temperature.

– Geographical parameters can be provided to create a regional subset of the *gbif4crest* dataset that is adapted to the studied data. These can include minimum and maximum longitude and latitude (`xmn`, `xmx`, `ymn`, `ymx`), continent, ocean or country names (see `accCountryNames()` and `accBasinNames()` for a list of accepted names), and also some ecological classifiers, such as realms, biomes or ecoregions (see `accRealmNames()` for a list of accepted names).

315 Only the occurrences that respect all the specified constraints will be returned.

– To estimate reliable PDFs, it is recommended to use at least 20 distinct occurrences for each species, but different values can be specified with the `minGridCell` parameter.

– Optional information about the site, such as a name and coordinates, can be provided and, where possible, this information will be represented on the different graphical diagnostic tools created by *crestr* (*e.g.* the location of the record can be added to the maps if the coordinates are provided).

320

```
rcnstrctn <- crest.get_modern_data(  
  df = MD96_2048,  
  pse = PSE,  
  selectedTaxa = selectedTaxa,  
325  taxaType = 1,  
  climate = c('bio1'),  
  xmn = NA, xmx = NA,  
  ymn = -35, ymx = NA,  
  continents = 'Africa',  
330  countries = c('South Africa', 'Kenya',  
    'Lesotho', 'eSwatini', 'Botswana',  
    'Mozambique', 'Zimbabwe', 'Zambia',  
    'Malawi', 'Tanzania', 'Namibia',  
    'Uganda', 'Rwanda', 'Burundi'),  
335  realms = NA,  
  biomes = NA,
```



```
ecoregions = NA,  
minGridCells = 20,  
site_info = c(34.0167, -26.1667),  
340 site_name = 'MD96-2048',  
dbname = "gbif4crest_02",  
verbose = TRUE  
)
```

The `crest.get_modern_data()` function reads all the data and parameters, extracts the data from the cloud-based  
345 *gbif4crest* database, processes the distribution data and returns everything as a structured `crestObj` — here called `rcnstrctn`;  
Fig. 5 — that will be read and modified by all subsequent functions. Alternatively, the function `crest.set_modern_data()`  
could be called instead of `crest.get_modern_data()` to use personal calibration data instead of the *gbif4crest* database.  
If the calibration data needed for this study were available as a `distributions` and `climate_space` data frames (Section  
3.3), similar results would be obtained using the following command:

```
350 rcnstrctn <- crest.set_modern_data(  
df = MD96_2048,  
distributions = distributions,  
climate_space = climate_space,  
selectedTaxa = selectedTaxa,  
355 climate = c('biol'),  
weight = FALSE,  
minGridCells = 20,  
site_info = c(34.0167, -26.1667),  
site_name = 'MD96-2048',  
360 verbose = TRUE  
)
```

### 4.3 Estimating the climate responses (the PDFs)

The probabilistic proxy-climate relationships, *i.e.* the PDFs, are estimated from the presence data using the `crest.calibrate()`  
function. As described in section 2.1.1, the different parameters should be carefully considered to produce reliable PDFs. These  
365 include specifying:

- the shape of the species PDFs, which should be either ‘normal’ or ‘lognormal’, depending on the variable to reconstruct.
- the width of the climate bins (`bin_width`) expressed in the variables’ units (*e.g.* 2°C or 50 mm) if the PDFs have corrected for an heterogenous climate space (`climateSpaceWeighting` set to `TRUE`). Dividing the total climate space in 15-25 bins often leads to good results, but other values are possible.



- 370 – the number of intervals required to divide the studied climate range and fit the PDFs `npoints`. This will ultimately define the climate resolution of the reconstructions. `crest_r` runs faster with a lower resolution but this can lead to a problem of aliasing of the reconstructions.
- set `geoWeighting` to `TRUE` if the species PDFs of the different composing species should be weighted according to the square-root of the extent of their modern distribution.

```
375 rcnstrctn <- crest.calibrate(  
  rcnstrctn,  
  shape = c('normal'),  
  climateSpaceWeighting = TRUE,  
  bin_width = c(2),  
380  npoints = 500,  
  geoWeighting = TRUE,  
  verbose = TRUE  
)
```

#### 4.4 Assessing the coherency of the climate space and climate responses

385 In every study involving estimating relationships between biological entities and environmental parameters, the first step is always to ensure that the defined calibration dataset is as coherent as possible. This includes ensuring that 1) all the important taxa are present, and their distribution is not truncated, 2) the climate values to reconstruct are likely to be in the study area (the reconstructions are bounded by the lowest and highest values observed in the modern climate space) and 3) there is no large sampling or representativity bias (*e.g.* along country borders due to different sampling efforts). Ideally, the climate sampling  
390 should be as homogeneous as possible, even if the extreme climate values will always be under-represented compared to the median ones. Equally importantly, the occurrence data across that space should be similarly distributed to ensure a proper sampling of the climate space. However, deviations from a theoretical one-to-one (or at least proportional) equivalence between climate and occurrence data abundance are not necessarily a bad characteristic. In our case study, the spatial variability represent  
395 (Myers et al., 2000). All these elements should be checked and accounted for while designing the final calibration dataset.

The ‘climateSpace’ graphical diagnostic tool was thus designed for a rapid assessment of all these characteristics (Fig. 6). This diagnostic figure is also very important to identify potential local or global correlations between different climate variables and assess the risks of confounding variables (Juggins (2013), Chevalier et al. (2020b)). Any change to any of the parameters related to the definition of the climate space (study area, climate variables to reconstruct) will require to re-run  
400 `crest.get_modern_data()` or `crest.set_modern_data()` with updated parameters and/or data.

```
plot_climateSpace(rcnstrctn, save=TRUE,  
  filename='Figure 6.png',
```



```
as.png=TRUE, png.res=600,  
width=6.9, height=4.4,  
405 y0=0.4,  
add_modern=TRUE  
)
```

With the study area and climate space defined, the next step is to search for taxa that show specific relationships with climate. While all species eventually respond to all climate variables, within a given region they can be more sensitive to one  
410 over another. The low taxonomic resolution of some fossil proxies, such as pollen data, can also mask strong species-climate relationships. Looking at each individual climate response(s) and assessing their significance within the boundary conditions of the study is thus critical. The ‘taxaCharacteristics’ diagnostic plot was designed for this task (Fig. 7). One summary plot can be generated for each taxon, where the geographical distributions and climate responses can be assessed and inter-compared.

As illustrated in Fig. 7, Ericaceae is preferentially observed in the colder environments of the study area, its higher per-  
415 centages occur during glacial periods, and a coherent response of all its composing species can be observed despite a high diversity (141 species with at least 20 unique occurrences across the study area). All these elements indicate that Ericaceae can be considered as an indicator of colder environmental conditions in eastern and southern Africa. Sensitivities to other variables can also be expected but are not considered in this study. Making such sensitivity inferences can be key to define a list of taxa that can be used to reconstruct temperature (Chevalier and Chase (2015), Chevalier et al. (2021)), but also to support qualitative  
420 interpretations of palaeoecological datasets (Chevalier et al. (in press), Quick et al. (2021)).

```
plot_taxaCharacteristics(rcnstrctn,  
taxanames='Ericaceae', save = TRUE,  
filename = 'Figure 7.png',  
as.png=TRUE, png.res=600,  
425 width=6.9, height=8.13,  
add_modern=TRUE  
)
```

Another useful diagnostic plot is the ‘violinPDFs’ (Fig. 8) that represents the PDFs of a selection of taxa on the same scale, which helps comparing the different responses. All the violins have the same area (all the probabilities sum to 1) and the  
430 taxa are ranked by increasing value of their temperature optima (*i.e.* the temperature corresponding to the peak of the PDF). However, due to the possible multimodality of the PDFs and differences in tolerance ranges, this ranking does not mean that a taxon on the left always represents colder conditions than a taxon on the right. This is illustrated in many ways on Fig. 8 with, for example, *Cassia*-type that is estimated to experience warmer conditions than *Coffea*-type ~61% of the time (based on 100,000 random draws from their respective PDFs) despite having a ‘colder’ climate optimum, or *Diospyros* that can tolerate  
435 much warmer conditions than most taxa with warmer optima. This type of representation can be particularly helpful to have objective interpretations of ecological changes from pollen diagrams (Chevalier et al., in press, Quick et al. (2021)).

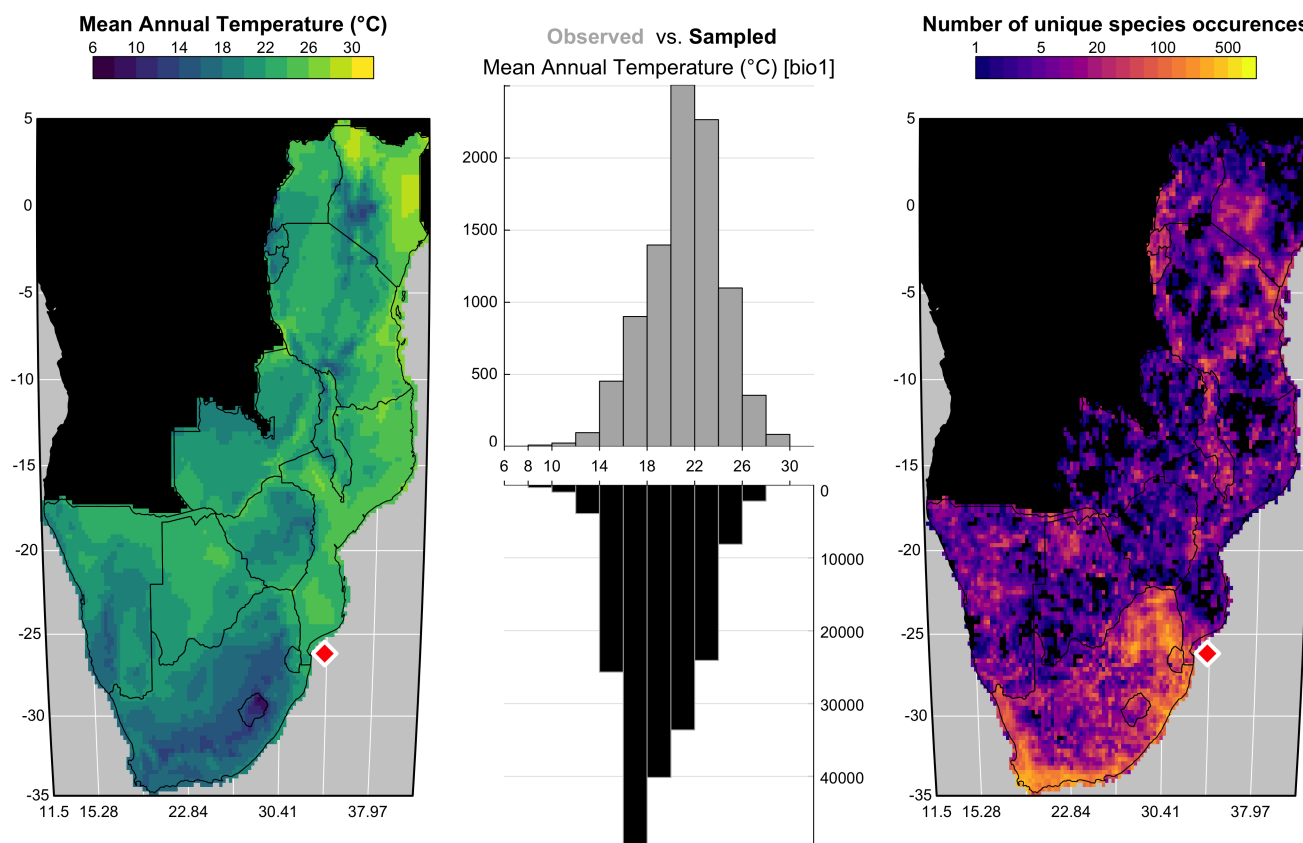


**Figure 6.** 'climateSpace' graphical diagnostic tool to evaluate the calibration dataset. The map on the right represents the density of unique species occurrences in each grid cell, here highlighting a certain bias towards South Africa. The lower abundance of plant data available from Angola and the Democratic Republic of Congo (data not shown) is the reason why these two countries were excluded from the study area. The map on the left represents the studied climate variable (MAT) across the study area. The double histogram in the middle represents the distribution of MAT (in grey, top), while the black histogram (bottom) represents how this distribution is sampled by the calibration data. Differences between the two histograms can be used to identify biases in the calibration dataset. Here, the small shift of the black histograms towards colder values (towards the left) is another way of seeing that more data are available from South Africa than other countries and reflects the regional patterns of biodiversity. If more variables had been selected in this study, additional rows would be added to the figure with a similar climate map and histograms and a scatterplot of the climate variables to highlight potential local or regional modern correlations.

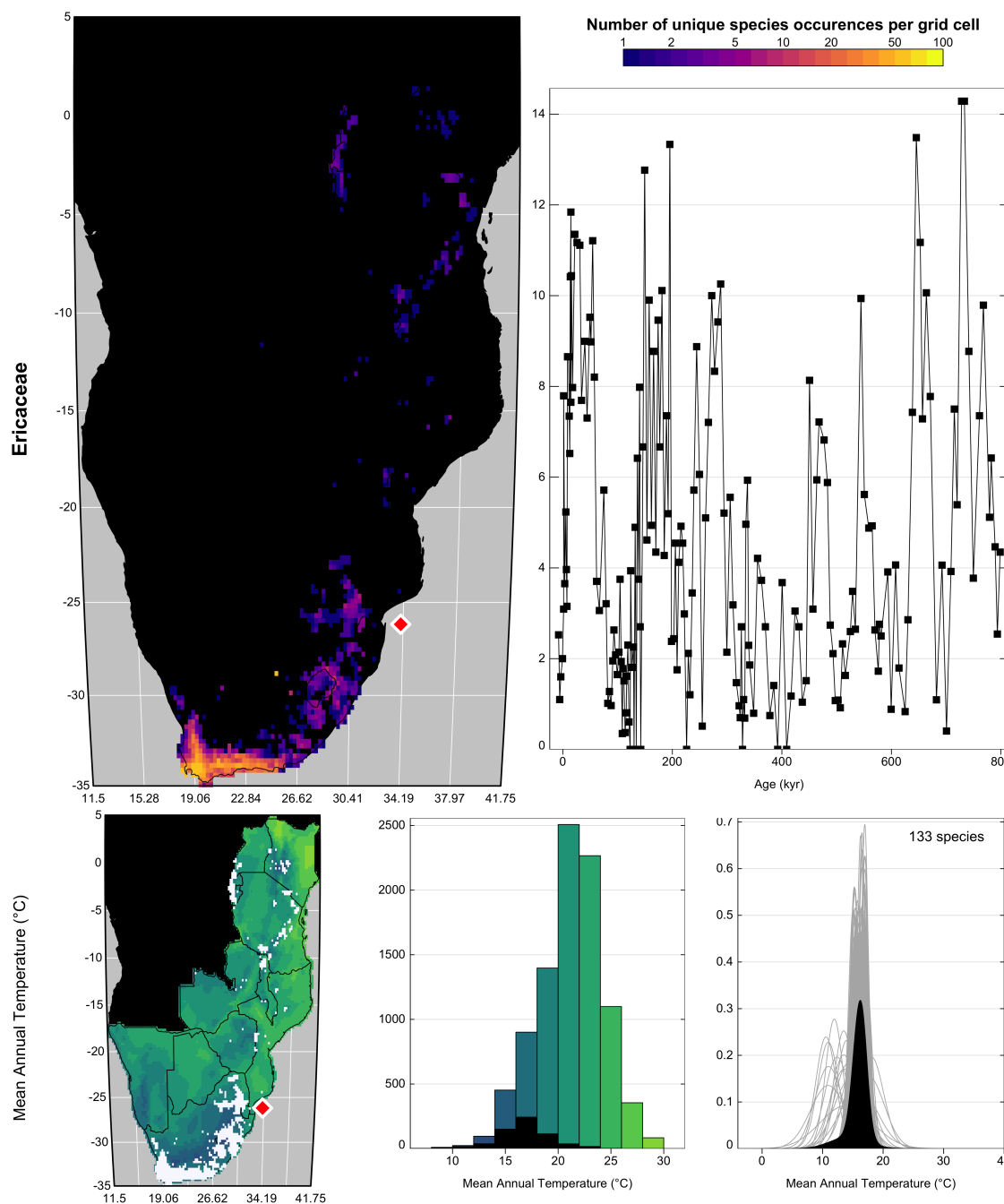


**Figure 7.** 'taxaCharacteristics' graphical diagnostic tool to assess the sensitivity of taxa to climate. In the top row, the map represents the density of unique species occurrences per grid cell and the time series represents the variability of the taxon against time or depth. The bottom row is specific to each selected variable (only one row in this case), where the map represents the geographical distribution of the taxon (in white) against the climate background, the histogram represents the climate space (in colour) and how this climate is sampled by the taxon (in black) and finally the right plot represents the climate response of the taxon (in black) as well as the response of all the composing species (in grey). This diagram shows that Ericaceae is preferentially associated with colder temperatures in the study area. The red diamond indicates the location of the studied record.

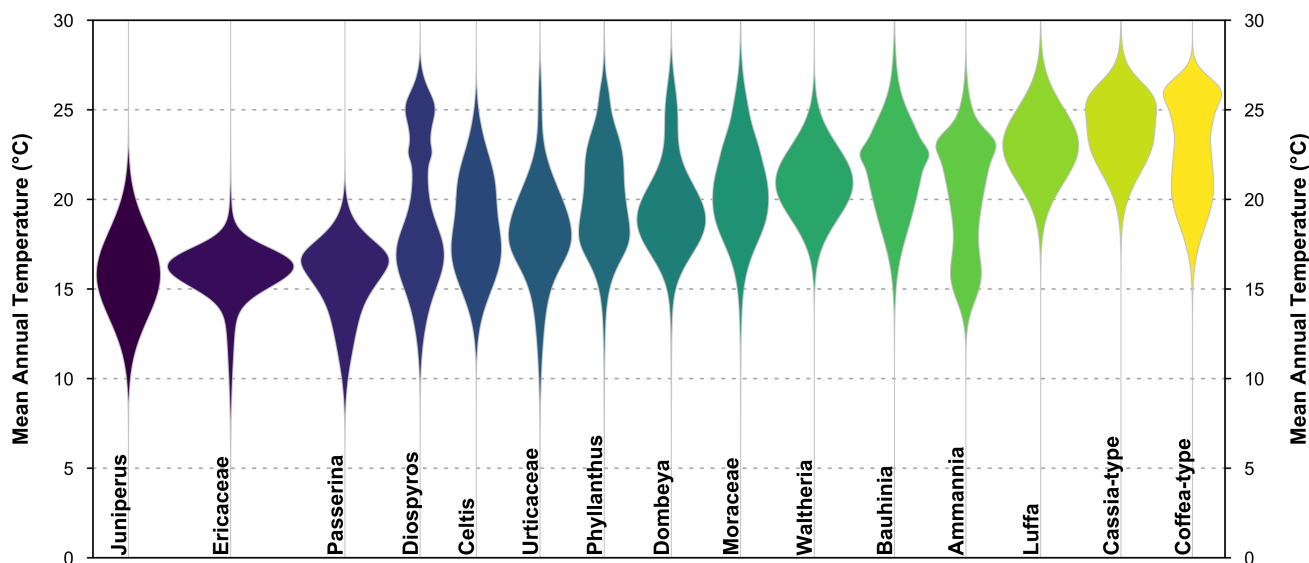


**Figure 8.** 'violinPDFs' graphical diagnostic tool to represent the PDFs of various taxa (here only a subset of 15). The taxa are sorted and colour coded by their temperature optima (i.e. the temperature corresponding to the peak of their PDFs).

```
tax <- sample(rcnstrctn$input$taxa.name,  
             15)  
plot_violinPDFs(rcnstrctn,  
440   taxanames = tax,  
       save = TRUE,  
       filename = 'Figure 8.png',  
       as.png=TRUE, png.res=600,  
       width = 6.9, height = 3,  
445   ylim=c(0,30)  
)
```

#### 4.5 Reconstructing climate

Along with the `df` data frame provided to the `crest.get_modern_data()` or `crest.set_modern_data()` functions, a set of reconstruction parameters have to be chosen to combine PDFs and estimate climate parameters. The `selectedTaxa`  
450 data frame that is stored in the `crestObj` (see Fig. 5) defines the taxa that will be used to reconstruct each climate variable (by default, all taxa are included if sufficient data are available to fit a PDF). This selection can be modified by using the `includeTaxa()` and `excludeTaxa()` functions. Here for instance, both `Aizoaceae` and `Chenopodiaceae/Amaranthaceae` were excluded because they are not primarily sensitive to temperature in southern Africa.



```
rcnstrctn <- excludeTaxa(rcnstrctn,  
455   taxa=c('Aizoaceae',  
          'Chenopodiaceae/Amaranthaceae'),  
        climate=c('biol')  
)
```

Climate reconstructions are performed by the `crest.reconstruct()` function. A minimum 'presence threshold' below  
460 which the taxa will be always considered absent can also be provided to reduce the noise of the fossil dataset (*e.g.* pollen percentages lower than 1 or 2% are commonly excluded from reconstructions, Chevalier et al. (2020b)). If `presenceThreshold` is set to zero as is the case here, all the strictly positive pollen percentages are considered as true presences and used accordingly to reconstruct MAT. To weight the taxa as described in Eq. 7, four options are available in `crest`:

- 465 – The data can be converted to presence/absence with all the values above and below `presenceThreshold` being changed to ones and zeros, respectively. This option is recommended for data such as macrofossils for which relative abundances cannot be reliably estimated.
- The data can be converted to percentages to weight the taxa according to their relative abundance. This option is recommended for data where reliable and direct proportions can be estimated.
- 470 – The data can be normalised following the method proposed by Chevalier et al. (2014) and described here by Eq. 8. This option is recommended for pollen data for instance.
- The data can be directly weighted by the values provided in `df`, which implies that users can define their own specific weighting strategy.

```
rcnstrctn <- crest.reconstruct(  
  rcnstrctn,  
475  presenceThreshold = 0,  
  taxWeight = "normalisation",  
  verbose = TRUE  
)
```

#### 4.6 Analysing and understanding the reconstruction(s)

480 Characterising the most important factors underlying a reconstruction is often complex. In this section, I present three different graphical diagnostic tools that provide different perspectives on the reconstructed data and help opening the statistical black box in a visual way. First, the full probabilistic breadth of the reconstructions can be represented by using the standard `R plot()` function, which has been adapted to plot data stored in a `crestObj` (Fig. 9). While the probabilistic representation of the data should be preferred because it represents all the information available, a simpler version of this plot with the climate



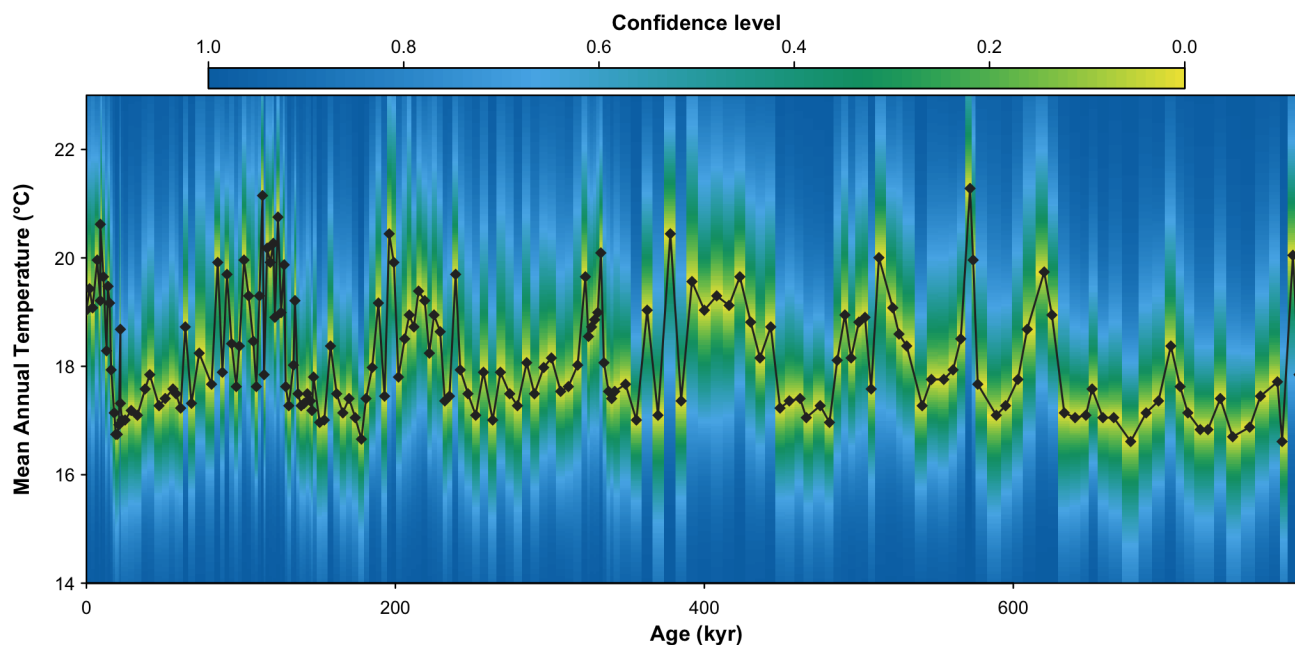


**Figure 9.** MAT probabilistic reconstructions for marine core MD96-2048. The yellow-green-blue colour gradient represents the uncertainties associated with each sample. This reconstruction is identical to the reconstruction presented in Chevalier et al. (2021) and the reader is referred to this publication for an in-depth validation and discussion of these results.

485 optima and more common uncertainty ranges represented as colour bands can be obtained by specifying `simplify=TRUE`  
(not shown).

```
plot(rcnstrctn,  
     filename='Figure 9.png',  
     save=TRUE,  
490  as.png=TRUE, png.res=600,  
     width=6.9, height=3.54,  
     ylim=c(14,23), uncertainties=1,  
     simplify=FALSE,  
     col=plot3D::gg2.col(200)[1:100],  
495  pt.cex=0.8, pt.lwd=1, pt.col='#2c2c2c'  
)
```

The `plot_combinedPDFs()` function can then be used to identify the taxa that are driving the reconstruction by focusing on the sample level (Fig. 10). In this plot, the PDFs of all the taxa present in the sample and selected to reconstruct the climate

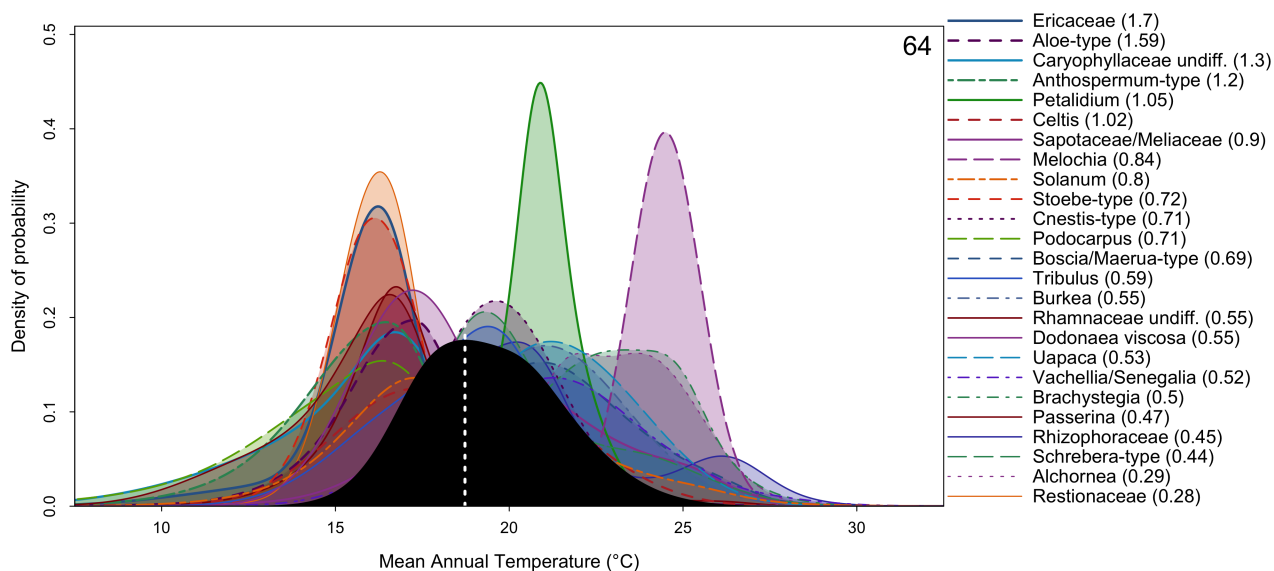


**Figure 10.** 'combinedPDFs graphical diagnostic tool that shows the combination of the PDFs of all the taxa recorded in a sample (in colour). The thickness of the lines is proportional to the weight of the taxa in the sample (absolute value indicated next to each taxon name). The black curve represents the posterior MAT reconstruction, from which a 'best' climate estimate can be estimated from the maximum of the curve and uncertainties derived by calculating the area under the curve.

variable are represented along with the reconstruction. This type of plot can help identify if there is a particular PDF that is at odds with the general assemblage, which can be indicative of a confounding factor. It is also useful to visualise the full spread of the uncertainties and, by extension, highlight that reconstructions can be multimodal. The presence of multimodality can be the underlying cause of apparent noise in the reconstructions because minor changes in the taxa composition or percentages can force the system to oscillate between two maxima and thus 'appear' noisy, even if the background rate of change is minor. This can also be seen from the reconstruction plot if the full uncertainties are represented (`simplify=FALSE`).

```

505 plot_combinedPDFs(rcnstrctn,
    samples=3, only.present=TRUE,
    only.selected=TRUE, save = TRUE,
    filename = 'figure 10.png',
    as.png=TRUE, png.res=600,
510 width=6.9, height=3,
    xlim=c(7.5, 32.5)
)

```

Finally, a standard post-processing analysis of CREST reconstructions is a form of leave-one-out (LOO) analysis that is done with the `loo()` function. In the CREST context, a LOO analysis consists in repeatedly 'unselecting' one taxon at a time,



515 re-running the reconstruction without that taxon and measuring the associated reconstruction anomalies. A detailed analysis of  
the results can contribute to a deeper insight regarding which taxa are the most important in driving the reconstructed climate  
signal. Taxa that exhibit large LOO values indicate that they have a large influence on the reconstruction. However, it does not  
necessarily mean that they are strong climate indicators. Large LOO values can arise when the PDFs are biased by unaccounted  
factors and are, as a result, at odds with the rest of the PDFs. Such factors can, for instance, include an incomplete estimate of  
520 the climate response, which induces a bias or shift of the climate preferences, or a sensitivity of the taxon to other climatic (*e.g.*  
aridity instead of temperature) or non-climatic (*e.g.* edaphic conditions) factors. In all cases, it is usually preferable to exclude  
such taxa from the reconstruction.

```
rcnstrctn <- loo(rcnstrctn,  
  verbose = TRUE
```

525 )

The LOO analysis is a powerful tool to understand the taxa that primarily drive the reconstruction and the LOO results can be  
represented as a common stratigraphic diagram, where each row represents the effect of removing a taxon from the reconstruc-  
tion (Fig. 11). For example, the expected net cold effect of including Ericaceae in the MAT reconstructions from MD96-2048  
pollen record is immediately visible on Fig. 11. Similarly, the effect of removing either Ericaceae or Caryophyllaceae undiff.  
530 from the sample dated at 64 kyr (represented on Fig. 10) is quite strong with a net warming of 1.19 and 0.44°C, respectively.  
This type of plot can thus be used for both global and sample-specific inferences about the drivers of the reconstruction. De-  
pending on the vegetation composition, some taxa can even sometimes be categorised as cold indicators when the assemblage  
represents warm conditions, or warm indicators when the assemblage represents cold conditions (*e.g. Hypoestes/Dicliptera-*  
type on Fig. 11).

```
535 tax <- rcnstrctn$inputs$taxa.name[6:25]
```

```
plot_loo(rcnstrctn,  
  taxanames=tax,  
  xlim=c(0, 340), save = TRUE,  
  filename = 'Figure 11.png',  
540  as.png=TRUE, png.res=600,  
  width=3.5, height=8,  
  bar_width=3, col_neg='coral3',  
  col_pos='darkcyan'  
)
```

#### 545 4.7 A wrapper function

To simplify the use of the package, the three stages of the reconstruction process – data acquisition (`crest.get_modern_data()`  
or `crest.set_modern_data()` if the *gbif4crest* dataset is not used [not shown]), calibration (`crest.calibrate()`)

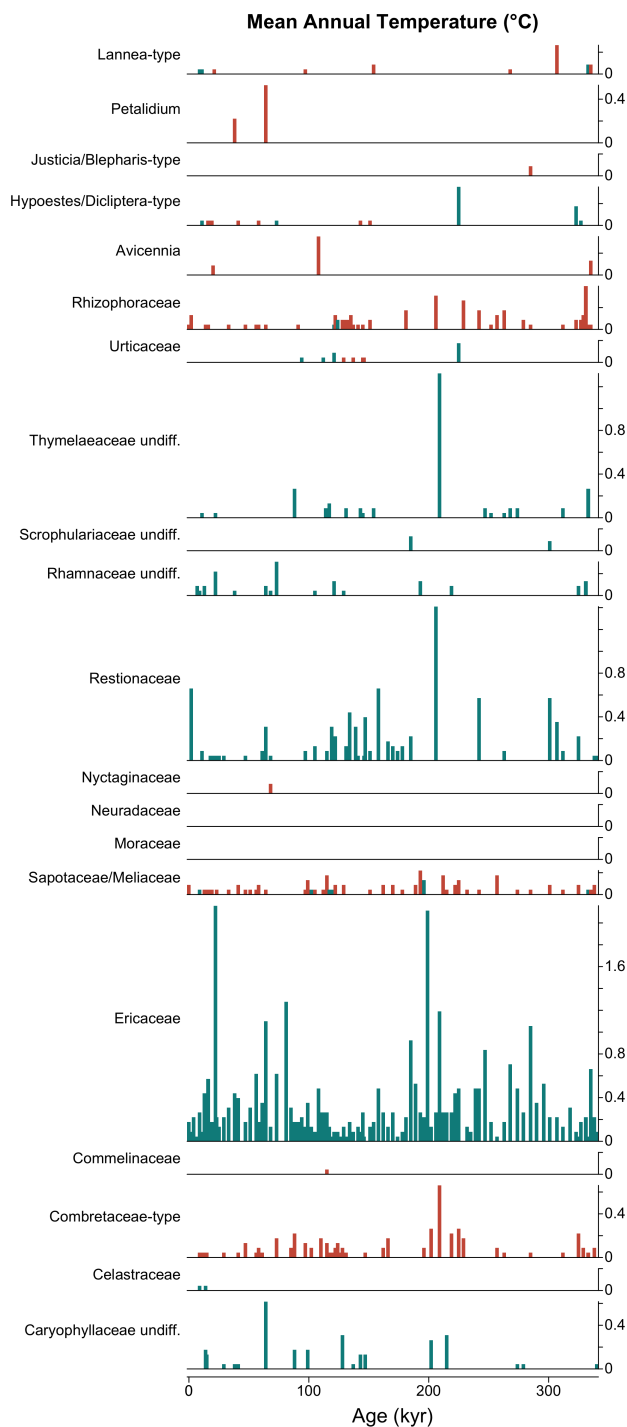


**Figure 11.** Leave-one-out (LOO) graphical diagnostic tool to illustrate the influence of different taxa on the reconstructions. Here, the results are only showed for a subset of the taxa observed in marine core MD96-2048 (only 20 out of the 171 available taxa are represented). The height of each bar represents the net effect (in °C) of removing the taxon from the reconstruction. The colours indicate the sign of the anomaly with blue (cf. Ericaceae) and red (cf. Combretaceae-type) taxa being cold and warm indicators in this setting, respectively.



and reconstruction (`crest.reconstruct()`) – can be called in one line of code using the wrapper function `crest()`. This function takes the same parameters described for the ‘step-by-step’ functions with the same default values and may be preferred, for instance, when reconstructing several records at the same time.

#### 4.8 Exporting the reconstructions

All the data stored in the `crestObj` can be easily exported from the R environment as spreadsheets and RData files using either `export_pdfs()` to save the climate responses of the studied taxa, or `export()` to save the reconstructions and many associated data in a publishable format. The latter also saves the `crestObj` as an RData file for easy reloading and/or sharing of the data.

```
export(rcnstrctn,  
      loc='path/to/folder',  
      fullPosterior = TRUE,  
      loo = TRUE,  
      weights = TRUE,  
      pdfs = TRUE  
)
```

#### 4.9 Citing building elements

Finally, all the reconstructions derived from `crestr` are built on numerous, independent research efforts, including data compilations, modelling projects, statistical developments and/or software engineering. To support the long-term development and/or support of all these building elements, it is crucial to always acknowledge all of them, even if their processing is mostly invisible to the users. As such, the list of references that must be cited for each use of `crestr` is automatically included in the summary tab of the spreadsheet generated by the `export()` function. In addition, the citation information can also be directly obtained from R using `cite_crest(rcnstrctn)`. The function looks at the type of data that were used (e.g. the subset of the GBIF data were used, which climate variables) and returns a corresponding list of references. For example, a simple way of crediting all the contributors for the MAT reconstruction from marine core MD96-2048 presented here could be the following: “To create this MAT reconstruction from the pollen record from marine core MD96-2048 (Dupont et al. (2019)), we employed the CREST method (Chevalier et al. (2014), Chevalier (2019)). The PDFs were estimated by combining the MAT field of Fick and Hijmans (2017) and the plant occurrence data of GBIF (GBIF (2020m), GBIF (2020k), GBIF (2020g)). The numerical analyses were realised with the `crestr` R package v1.0.0 (this reference).”

### 5 Perspectives and conclusion

CREST is a statistical method designed 1) to model probabilistic relationships between climate proxies and climate from modern observations and 2) to use these relationships to reconstruct past climate quantitatively. Initially, its use was enabled



by a python point-and-click graphical user interface to favour accessibility to a diverse spectrum of palaeoclimatologists,  
580 palaeoceanographers and palaeoecologists, including those with limited coding experience (Chevalier et al., 2014). However,  
such accessibility limited flexibility and how the method could be most effectively employed. Therefore, this article introduces  
an open-source R package to use CREST in a programmatic environment. The benefits of this transition are significant and  
include scriptability (*i.e.* the possibility of analysing many records automatically and sequentially), reproducibility (*i.e.* the  
capacity to reproduce an analysis) and better inter-operability (*i.e.* R packages are compatible with all computer systems).  
585 However, maintaining the highest level of accessibility remained at the core of the development process and is illustrated in  
the final product by the small number of functions necessary to run a complete analysis and by the suite of detailed graphical  
diagnostic figures.

The package is aimed at all researchers that are interested in using CREST to analyse palaeoecological datasets. In addition,  
its broad applicability will allow taking advantage of the recent growth of curated, open-access fossil datasets that created  
590 unprecedented opportunities to reconstruct climate from a wide range of proxies, particularly in regions where they are urgently  
needed. This package will also contribute to the current transition from single-site to multi-site studies that is necessary to  
better understand past climate dynamics. However, it is essential to remember that running such techniques on several datasets  
should be done carefully, as many factors can impact the reconstruction process. Calibration datasets and reconstructions  
should always be assessed, possibly against independent evidence when they are available, even if there is, unfortunately, no  
595 single way to validate a reconstruction (but see Chevalier et al. (2020b) for some discussions on the generic principles).

Over time, the `crestr` package will be enriched with new functionalities to facilitate reconstruction validation. The on-  
line documentation will also be updated with diverse examples and tutorials based on real applications and assessments  
(<https://mchevalier2.github.io/crestr/>). Finally, bug reports, feedback, and suggestions for newer functionalities and graph-  
ical diagnostic tools are encouraged and can be transmitted to the author directly or through GitHub's bug report portal  
600 (<https://github.com/mchevalier2/crestr/issues>).

*Code and data availability.* The `crestr` package is currently accessible from GitHub (<https://github.com/mchevalier2/crestr>), where I also  
welcome feedback and strongly encourage contributions and enhancements via the issue tracker (<https://github.com/mchevalier2/crestr/issues>).  
The package has also been submitted to CRAN. The data used for the example application (pollen record from marine core MD96-2048 and  
associated temperature reconstructions) can be accessed from <https://doi.pangaea.de/10.1594/PANGAEA.915923>.

605 *Competing interests.* The author declare no competing interests.

*Acknowledgements.* This research has been supported by the Swiss National Science Foundation (grant no. CRSK-2\_195875), with addi-  
tional support from the University of Lausanne. I thank Brian Chase, Yoshi Maezumi, Lynne Quick and, last but not least, Mine Altinli  
for their invaluable comments and suggestions on early versions of the manuscript. NOAA High Resolution SST data provided by the



NOAA/OAR/ESRL PSL, Boulder, Colorado, USA, from their Web site at <https://psl.noaa.gov/data/gridded/data.noaa.oisst.v2.highres.html>.  
610 And finally, I would also like to address a special thanks to the articles contributors for their Climate of the Past Rmarkdown template!



## References

- Birks, H. J. B., Heiri, O., Seppä, H., and Bjune, A. E.: Strengths and weaknesses of quantitative climate reconstructions based on Late-Quaternary biological proxies, *The Open Ecology Journal*, 3, 68–110, <https://doi.org/10.2174/1874213001003020068>, 2010.
- Bivand, R. and Rundel, C.: rgeos: Interface to Geometry Engine - Open Source ('GEOS'), <https://CRAN.R-project.org/package=rgeos>, r package version 0.5-5, 2020.
- Bivand, R., Keitt, T., and Rowlingson, B.: rgdal: Bindings for the 'Geospatial' Data Abstraction Library, <https://CRAN.R-project.org/package=rgdal>, r package version 1.5-23, 2021.
- Bivand, R. S., Pebesma, E., and Gomez-Rubio, V.: *Applied spatial data analysis with R*, Second edition, Springer, NY, <https://asdar-book.org/>, 2013.
- 620 Bray, P. J., Blockley, S. P., Coope, G. R., Dadswell, L. F., Elias, S. A., Lowe, J. J., and Pollard, A. M.: Refining mutual climatic range (MCR) quantitative estimates of palaeotemperature using ubiquity analysis, *Quaternary Science Reviews*, 25, 1865–1876, <https://doi.org/10.1016/j.quascirev.2006.01.023>, 2006.
- Castañeda, I. S., Caley, T., Dupont, L. M., Kim, J.-H., Malaizé, B., and Schouten, S.: Middle to Late Pleistocene vegetation and climate change in subtropical southern East Africa, *Earth and Planetary Science Letters*, 450, 306–316, <https://doi.org/10.1016/j.epsl.2016.06.049>, 2016.
- 625 Chase, B. M., Boom, A., Carr, A. S., Carré, M., Chevalier, M., Meadows, M. E., Pedro, J. B., Stager, J. C., and Reimer, P. J.: Evolving southwest African response to abrupt deglacial North Atlantic climate change events, *Quaternary Science Reviews*, 121, 132–136, <https://doi.org/10.1016/j.quascirev.2015.05.023>, 2015a.
- Chase, B. M., Lim, S., Chevalier, M., Boom, A., Carr, A. S., Meadows, M. E., and Reimer, P. J.: Influence of tropical easterlies in the southwestern Cape of Africa during the Holocene, *Quaternary Science Reviews*, 107, 138–148, 2015b.
- 630 Chevalier, M.: Enabling possibilities to quantify past climate from fossil assemblages at a global scale, *Global and Planetary Change*, 175, 27–35, <https://doi.org/10.1016/j.gloplacha.2019.01.016>, 2019.
- Chevalier, M.: GBIF database for CREST, <https://doi.org/10.6084/m9.figshare.6743207>, 2020.
- Chevalier, M. and Chase, B. M.: Southeast African records reveal a coherent shift from high- to low-latitude forcing mechanisms along the east African margin across last glacial–interglacial transition, *Quaternary Science Reviews*, 125, 117–130, <https://doi.org/10.1016/j.quascirev.2015.07.009>, 2015.
- 635 Chevalier, M. and Chase, B. M.: Determining the drivers of long-term aridity variability: a southern African case study, *Journal of Quaternary Science*, 31, 143–151, <https://doi.org/10.1002/jqs.2850>, 2016.
- Chevalier, M., Cheddadi, R., and Chase, B. M.: CREST (Climate REconstruction SofTware): a probability density function (PDF)-based quantitative climate reconstruction method, *Climate of the Past*, 10, 2081–2098, <https://doi.org/10.5194/cp-10-2081-2014>, 2014.
- 640 Chevalier, M., Chase, B. M., Quick, L. J., Dupont, L. M., and Johnson, T. C.: PANGAEA dataset associated with "Temperature change in subtropical southeastern Africa during the past 790,000 years", <https://doi.org/10.1594/PANGAEA.915923>, 2020a.
- Chevalier, M., Davis, B. A. S., Heiri, O., Seppä, H., Chase, B. M., Gajewski, K., Lacourse, T., Telford, R. J., Finsinger, W., Guiot, J., Kühl, N., Maezumi, S. Y., Tipton, J. R., Carter, V. A., Brussel, T., Phelps, L. N., Dawson, A., Zanon, M., Vallé, F., Nolan, C., Mauri, A., de Vernal, A., Izumi, K., Holmström, L., Marsicek, J., Goring, S. J., Sommer, P. S., Chaput, M., and Kupriyanov, D.: Pollen-based climate reconstruction techniques for late Quaternary studies, *Earth-Science Reviews*, 210, 103384, <https://doi.org/10.1016/j.earscirev.2020.103384>, 2020b.
- 645 Chevalier, M., Chase, B. M., Quick, L. J., Dupont, L. M., and Johnson, T. C.: Temperature change in subtropical southeastern Africa during the past 790,000 yr, *Geology*, 49, 71–75, <https://doi.org/10.1130/G47841.1>, 2021.





- Chevalier, M., Chase, B. M., Quick, L. J., and Scott, L.: An atlas of southern African pollen types and their climatic affinities, *Palaeoecology of Africa*, 35, <https://www.routledge.com/Quaternary-Vegetation-Dynamics-The-African-Pollen-Database/Runge-Gosling-Lezine-Scott/p/book/9780367755089>, in press.
- 650 Cordova, C. E., Scott, L., Chase, B. M., and Chevalier, M.: Late Pleistocene-Holocene vegetation and climate change in the Middle Kalahari, Lake Ngami, Botswana, *Quaternary Science Reviews*, 171, 199–215, <https://doi.org/10.1016/j.quascirev.2017.06.036>, 2017.
- Dupont, L. M., Caley, T., Kim, J.-H., Castañeda, I. S., Malaizé, B., and Giraudeau, J.: Glacial-interglacial vegetation dynamics in South Eastern Africa coupled to sea surface temperature variations in the Western Indian Ocean, *Climate of the Past*, 7, 1209–1224, <https://doi.org/10.5194/cp-7-1209-2011>, 2011.
- 655 Dupont, L. M., Caley, T., and Castañeda, I. S.: Effects of atmospheric CO<sub>2</sub> variability of the past 800 kyr on the biomes of southeast Africa, *Climate of the Past*, 15, 1083–1097, <https://doi.org/10.5194/cp-15-1083-2019>, 2019.
- Fick, S. E. and Hijmans, R. J.: WorldClim 2: new 1-km spatial resolution climate surfaces for global land areas, *International Journal of Climatology*, 37, 4302–4315, <https://doi.org/10.1002/joc.5086>, 2017.
- 660 Garcia, H. E., Weathers, K., Paver, C., Smolyar, I., Boyer, T., Locarnini, R., Zweng, M., Mishonov, A., Baranova, O., Seidov, D., and Reagan, J.: World Ocean Atlas 2018, Volume 3: Dissolved Oxygen, Apparent Oxygen Utilization, and Dissolved Oxygen Saturation., NOAA Atlas NESDIS 83, p. 38pp, 2019a.
- Garcia, H. E., Weathers, K., Paver, C., Smolyar, I., Boyer, T., Locarnini, R., Zweng, M., Mishonov, A., Baranova, O., Seidov, D., Reagan, J., and Others: World Ocean Atlas 2018. Vol. 4: Dissolved Inorganic Nutrients (phosphate, nitrate and nitrate+nitrite, silicate), NOAA Atlas NESDIS 84, p. 35pp, 2019b.
- 665 Garnier, Simon, Ross, Noam, Rudis, Robert, Camargo, Pedro, A., Sciaini, Marco, Scherer, and Cédric: viridis - Colorblind-Friendly Color Maps for R, <https://doi.org/10.5281/zenodo.4679424>, r package version 0.6.1, 2021.
- GBIF: GBIF: Global Biodiversity Information Facility, <https://www.gbif.org>, 2018.
- GBIF: Beetles occurrence data downloaded on September 24th, 2020, <https://doi.org/10.15468/dl.nteruy>, 2020a.
- 670 GBIF: Chironomids occurrence data downloaded on September 24th, 2020, <https://doi.org/10.15468/dl.jv3wsh>, 2020b.
- GBIF: Diatoms occurrence data downloaded on September 24th, 2020, <https://doi.org/10.15468/dl.vfr257>, 2020c.
- GBIF: Foraminifera occurrence data downloaded on September 24th, 2020, <https://doi.org/10.15468/dl.692yg6>, 2020d.
- GBIF: Rodentia occurrence data downloaded on September 24th, 2020, <https://doi.org/10.15468/dl.fscw6q>, 2020e.
- GBIF: Cycadopsidae occurrence data downloaded on September 24th, 2020, <https://doi.org/10.15468/dl.sfjz xu>, 2020f.
- 675 GBIF: Magnoliopsida occurrence data downloaded on September 24th, 2020, <https://doi.org/10.15468/dl.ra49dt>, 2020g.
- GBIF: Anthocerotopsida occurrence data downloaded on September 24th, 2020, <https://doi.org/10.15468/dl.t9zenf>, 2020h.
- GBIF: Gingkoopsida occurrence data downloaded on September 24th, 2020, <https://doi.org/10.15468/dl.da9wz8>, 2020i.
- GBIF: Gnetopsida occurrence data downloaded on September 24th, 2020, <https://doi.org/10.15468/dl.h2kjnc>, 2020j.
- GBIF: Liliopsida occurrence data downloaded on September 24th, 2020, <https://doi.org/10.15468/dl.axv3yd>, 2020k.
- 680 GBIF: Lycopodiopsida occurrence data downloaded on September 24th, 2020, <https://doi.org/10.15468/dl.ydhyhz>, 2020l.
- GBIF: Pinopsida occurrence data downloaded on September 24th, 2020, <https://doi.org/10.15468/dl.x2r7pa>, 2020m.
- GBIF: Polypodiopsida occurrence data downloaded on September 24th, 2020, <https://doi.org/10.15468/dl.87tbp6>, 2020n.
- GBIF: Bryophyta occurrence data downloaded on August 2nd, 2021, <https://doi.org/10.15468/DL.WD527G>, 2021a.
- GBIF: Marchantiophyta occurrence data downloaded on August 2nd, 2021, <https://doi.org/10.15468/DL.M2SSE4>, 2021b.
- 685 Hijmans, R. J.: raster: Geographic Data Analysis and Modeling, <https://CRAN.R-project.org/package=raster>, r package version 3.4-13, 2021.



- Hui, Z., Zhou, X., Chevalier, M., Wei, X., Pan, Y., and Chen, Y.: Miocene East Asia summer monsoon precipitation variability and its possible driving forces, *Palaeogeography, Palaeoclimatology, Palaeoecology*, 581, 110 609, <https://doi.org/10.1016/j.palaeo.2021.110609>, 2021.
- Juggins, S.: Quantitative reconstructions in palaeolimnology: new paradigm or sick science?, *Quaternary Science Reviews*, 64, 20–32, <https://doi.org/10.1016/j.quascirev.2012.12.014>, 2013.
- 690 Kühl, N., Gebhardt, C., Litt, T., and Hense, A.: Probability Density Functions as Botanical-Climatological Transfer Functions for Climate Reconstruction, *Quaternary Research*, 58, 381–392, <https://doi.org/10.1006/qres.2002.2380>, 2002.
- Lim, S., Chase, B. M., Chevalier, M., and Reimer, P. J.: 50,000 years of climate in the Namib Desert, Pella, South Africa, *Palaeogeography, Palaeoclimatology, Palaeoecology*, 451, 197–209, <https://doi.org/10.1016/j.palaeo.2016.03.001>, 2016.
- Lincoln, M.: clipr: Read and Write from the System Clipboard, <https://CRAN.R-project.org/package=clipr>, r package version 0.7.1, 2020.
- 695 Locarnini, R., Mishonov, A., Baranova, O., Boyer, T., Zweng, M., Garcia, H. E., Reagan, J., Seidov, D., Weathers, K., Paver, C., Smolyar, I., and Others: World ocean atlas 2018, volume 1: Temperature, NOAA Atlas NESDIS 81, p. 52pp, 2019.
- Myers, N., Mittermeier, R. A., Mittermeier, C. G., da Fonseca, G. A. B., and Kent, J.: Biodiversity hotspots for conservation priorities, *Nature*, 403, 853–858, <https://doi.org/10.1038/35002501>, 2000.
- Overpeck, J. T., Webb III, T., and Prentice, I. C.: Quantitative interpretation of fossil pollen spectra: Dissimilarity coefficients and the method of modern analogs, *Quaternary Research*, 23, 87–108, [https://doi.org/10.1016/0033-5894\(85\)90074-2](https://doi.org/10.1016/0033-5894(85)90074-2), 1985.
- 700 Pebesma, E. J. and Bivand, R. S.: Classes and methods for spatial data in R, *R News*, 5, 9–13, <https://CRAN.R-project.org/doc/Rnews/>, 2005.
- Quick, L. J., Chase, B. M., Carr, A. S., Chevalier, M., Grobler, B. A., and Meadows, M. E.: A 25,000 year record of climate and vegetation change from the southwestern Cape coast, South Africa, *Quaternary Research*, pp. 1–18, <https://doi.org/10.1017/qua.2021.31>, 2021.
- R Core Team: R: A Language and Environment for Statistical Computing, R Foundation for Statistical Computing, Vienna, Austria, <https://www.R-project.org/>, 2020.
- 705 R Special Interest Group on Databases (R-SIG-DB), Wickham, H., and Müller, K.: DBI: R Database Interface, <https://CRAN.R-project.org/package=DBI>, r package version 1.1.1, 2021.
- Reynolds, R. W., Smith, T. M., Liu, C., Chelton, D. B., Casey, K. S., and Schlax, M. G.: Daily high-resolution-blended analyses for sea surface temperature, *Journal of Climate*, 20, 5473–5496, <https://doi.org/10.1175/2007JCLI1824.1>, 2007.
- 710 Schauburger, P. and Walker, A.: openxlsx: Read, Write and Edit xlsx Files, <https://CRAN.R-project.org/package=openxlsx>, r package version 4.2.3, 2020.
- Soetaert, K.: plot3D: Plotting Multi-Dimensional Data, <https://CRAN.R-project.org/package=plot3D>, r package version 1.4, 2021.
- ter Braak, C. J. F. and van Dame, H.: Inferring pH from diatoms: a comparison of old and new calibration methods, *Hydrobiologia*, 178, 209–223, <https://doi.org/10.1007/BF00006028>, 1989.
- 715 ter Braak, C. J. F., Juggins, S., Birks, H. J. B., and van der Voet, H.: Weighted averaging partial least squares regression (WA-PLS): Definition and comparison with other methods for species-environment calibration, *Multivariate Environmental Statistics*, pp. 525–560, <https://doi.org/10.1007/BF00028046>, 1993.
- Wickham, H.: The Split-Apply-Combine Strategy for Data Analysis, *Journal of Statistical Software*, 40, 1–29, <http://www.jstatsoft.org/v40/i01/>, 2011.
- 720 Wickham, H.: stringr: Simple, Consistent Wrappers for Common String Operations, <https://CRAN.R-project.org/package=stringr>, r package version 1.4.0, 2019.
- Wickham, H. and Hesselberth, J.: pkgdown: Make Static HTML Documentation for a Package, <https://CRAN.R-project.org/package=pkgdown>, r package version 1.6.1, 2020.



- 725 Wickham, H. and Seidel, D.: scales: Scale Functions for Visualization, <https://CRAN.R-project.org/package=scales>, r package version 1.1.1, 2020.
- Wickham, H., Hester, J., and Chang, W.: devtools: Tools to Make Developing R Packages Easier, <https://CRAN.R-project.org/package=devtools>, r package version 2.3.2, 2020.
- Wickham, H., Ooms, J., and Müller, K.: RPostgres: 'Rcpp' Interface to 'PostgreSQL', <https://CRAN.R-project.org/package=RPostgres>, r package version 1.3.3, 2021.
- 730 Wright, K.: pals: Color Palettes, Colormaps, and Tools to Evaluate Them, <https://CRAN.R-project.org/package=pals>, r package version 1.7, 2021.
- Yi, S., Jun, C. P., nam Jo, K., Lee, H., Kim, M. S., Lee, S. D., Cao, X., and Lim, J.: Asynchronous multi-decadal time-scale series of biotic and abiotic responses to precipitation during the last 1300 years, *Scientific Reports*, 10, 1–10, <https://doi.org/10.1038/s41598-020-74994-x>, 2020.
- 735 Zomer, R. J., Trabucco, A., Bossio, D. A., and Verchot, L. V.: Climate change mitigation: A spatial analysis of global land suitability for clean development mechanism afforestation and reforestation, *Agriculture, Ecosystems & Environment*, 126, 67–80, <https://doi.org/10.1016/j.agee.2008.01.014>, 2008.
- Zweng, M., Seidov, D., Boyer, T., Locarnini, R., Garcia, H. E., Mishonov, A., Baranova, O., Weathers, K., Paver, C., Smolyar, I., and Others: World Ocean Atlas 2018, Volume 2: Salinity, NOAA Atlas NESDIS 82, p. 50pp, 2018.